

Re-examining the membership and origin of the ϵ Cha association

Simon J. Murphy^{1,2*}, Warrick A. Lawson³ and Michael S. Bessell²

¹ *Gliese Fellow, Astronomisches Rechen-Institut, Zentrum für Astronomie der Universität Heidelberg, Germany 69120*

² *Research School of Astronomy and Astrophysics, Australian National University, Canberra, ACT 2611, Australia*

³ *School of Physical, Environmental and Mathematical Sciences, University of New South Wales, Canberra, ACT 2600, Australia*

17 March 2019

ABSTRACT

We present a comprehensive investigation of the ϵ Chamaeleontis association (ϵ Cha), one of several stellar groups in the southern sky kinematically linked to the Scorpius-Centaurus OB association (Sco-Cen). We reassess the putative membership of ϵ Cha using the best-available proper motions (*Hipparcos*, Tycho-2 and SPM4) with radial velocity and lithium data from the literature and new ANU 2.3-m/WiFeS spectroscopy. After applying a kinematic convergence analysis our final membership comprises 35–41 stars from B9 to mid-M spectral types, with a mean distance of 110 ± 7 pc and a mean space motion of $(U, V, W) = (-10.9 \pm 0.8, -20.4 \pm 1.3, -9.9 \pm 1.4)$ km s⁻¹. Theoretical evolutionary models suggest ϵ Cha is 3–5 Myr old, distinguishing it as the youngest association in the solar neighbourhood and the only one associated with molecular material. Considering all the available evidence we reject several stars proposed as members in the literature and suggest they may belong to the background Cha I and II clouds or other nearby young groups. Our analysis underscores the importance of a holistic and conservative approach to assigning young stars to kinematic groups, many of which have only subtly different properties and ill-defined memberships. Fifteen ϵ Cha members show 3–22 μ m spectral energy distributions attributable to circumstellar discs, including 11 stars which appear to be actively accreting. Multi-epoch spectroscopy reveals three M-type members with broad and highly-variable H α emission as well as several new spectroscopic binaries. We conclude with a brief discussion of ϵ Cha’s connection to the young open cluster η Cha and the Lower Centaurus Crux (LCC) subgroup of Sco-Cen. Contrary to earlier studies which assumed η and ϵ Cha are coeval and were born in the same location, we find the groups were separated by ~ 30 pc when η Cha formed first in the outskirts of LCC 4–8 Myr ago, 1–3 Myr before the majority of ϵ Cha members.

Key words: open clusters and associations: individual: ϵ Chamaeleontis – stars: pre-main sequence – stars: kinematics and dynamics – stars: formation – stars: low-mass

1 INTRODUCTION

Young stars in the solar neighbourhood are ideal laboratories for studying circumstellar discs and nascent planetary systems at high resolution and sensitivity. Well-characterised samples of stars with ages $\lesssim 10$ Myr are particularly important, as it is during these epochs that discs rapidly evolve from massive gas-rich systems capable of supporting accretion and the formation of giant planets, to more-quiet dusty debris discs which are the precursors of terrestrial planets. (Williams & Cieza 2011).

Nearby kinematic associations like those around the young stars TW Hydrae (age 8–10 Myr) and β Pictoris (~ 12 Myr) have proven fruitful targets for such work (Zuckerman & Song 2004; Torres et al. 2008). However, the majority of stars in these groups show signs their primordial discs are already evolved (Fedele et al. 2010; Simon et al. 2012). Like the nearby and simi-

larly young η Chamaeleontis open cluster (Mamajek et al. 1999), the 3–5 Myr-old ϵ Chamaeleontis association (Mamajek et al. 2000; Feigelson et al. 2003) is therefore ideally suited to studies of the rapid disc evolution taking place at these intermediate ages (Fang et al. 2013; Sicilia-Aguilar et al. 2009).

However, because of ϵ Cha’s greater distance (100–120 pc) compared to other nearby young groups, southern declination and position in the foreground of the Chamaeleon molecular cloud complex (170–210 pc, 2–4 Myr; Luhman 2008) it has suffered from somewhat of an identity crisis in the literature. Over 50 members of a putative kinematic group in the region have been proposed in the past fifteen years and there are several overlapping definitions of the group in the literature. Unfortunately, many candidates lack radial velocities necessary for confirming membership in a kinematic group and several stars have no spectroscopy at all. If ϵ Cha is a true coeval group then all of its members must have consistent age indicators (e.g. X-ray and H α emission, Li I depletion, elevated colour-magnitude diagram placement, low surface gravity;

* Corresponding author: murphy@ari.uni-heidelberg.de

Zuckerman & Song 2004) and space motions (via proper motions and radial velocities) consistent with being a comoving ensemble.

In this contribution we attempt to clarify the situation by critically re-examining the membership of ϵ Cha. The structure of the paper is as follows. In §2 we outline the various members proposed in the literature. The observed properties of these stars are described in §3, including new multi-epoch spectroscopy. After applying a convergence analysis (§4) we present the new membership of ϵ Cha in §5. The age of the association, its discs, T Tauri stars and binaries are discussed in §6. We conclude with a discussion of ϵ Cha's relationship to the nearby η Cha open cluster and their origin in the Scorpius-Centaurus OB association in §7 and §8.

2 ϵ CHA IN THE LITERATURE

The ϵ Cha association has existed in the literature in various guises for fifteen years. Frink et al. (1998) discovered several young *ROSAT* sources between the Cha I and II dark clouds (Fig. 2) with proper motions that placed them much closer to the Sun ($d \approx 90$ pc, their “subgroup 2”). Terranegra et al. (1999) subsequently identified 13 stars between the clouds with similar proper motions, which they claimed formed a distinct kinematic association. They derived a distance of 90–110 pc and an isochronal age of 5–30 Myr.

While investigating the young open cluster η Cha (Mamajek et al. 1999), Mamajek et al. (2000) also looked at stars in the vicinity of ϵ Cha and HD 104237. They identified eight stars with congruent proper motions and photometry, and used several with radial velocities and parallaxes to derive a space motion for the group.

Feigelson et al. (2003) then obtained *Chandra X-ray Observatory* snapshots of two fields around HD 104237, finding four low-mass companions to the Herbig Ae star at separations of 160–1700 au and three more spectroscopically-young mid-M stars at larger separations. Luhman (2004b) soon added another three lithium-rich low-mass stars in the vicinity. These 12 stars constitute the ‘classical’ membership of ϵ Cha.

In their review of young stars near the Sun, Zuckerman & Song (2004) proposed a ~ 10 Myr-old group surrounding (but not including) ϵ Cha and HD 104237 which they called ‘Cha-Near’. It included six new candidates and 11 stars from the memberships of Terranegra et al. (1999) and Mamajek et al. (2000). While Zuckerman & Song considered Cha-Near and the aggregate around ϵ Cha/HD 104237 to be separate groups, it is highly likely they are all members of the same spatially-extended comoving association.

Finally, while investigating the disk properties of Cha I members with the *Spitzer Space Telescope*, Luhman et al. (2008) identified four stars with proper motions consistent with membership in the ϵ Cha association defined by Feigelson et al. (2003), and several new *ROSAT* sources not previously attributed to ϵ Cha. Three of the seven new candidates had spectral energy distributions typical of accreting Classical T Tauri (CTT) stars.

2.1 Torres et al. (2008) compilation

Torres et al. (2008) reviewed ϵ Cha as part of their ongoing program to identify new members of young, local associations (see also Torres et al. 2006). Using radial velocities from the literature and their own observations, they proposed 24 high-probability ϵ Cha members with congruent kinematics, photometry and lithium absorption. Their solution included 14 stars compiled in previous

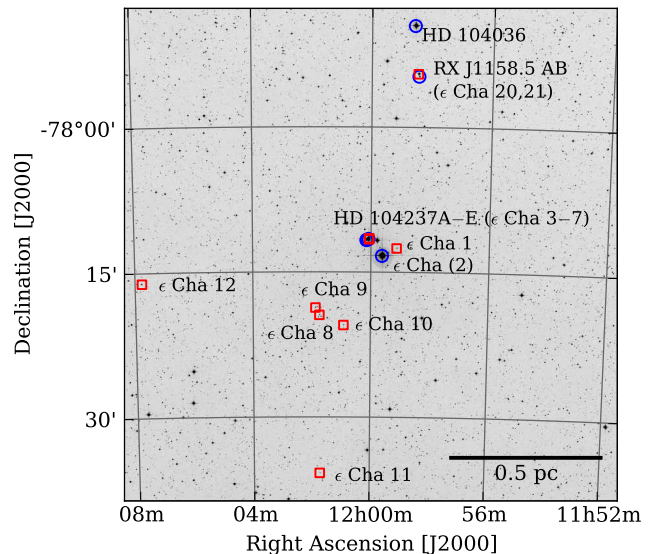


Figure 1. POSS2-IR 1 deg² image centred on ϵ Cha, with proposed members from the literature (red squares) and kinematic members from Torres et al. (2008) (blue circles). The scale uses the 111 pc distance to ϵ Cha.

studies above, six new members and four members of the open cluster η Cha (RECX 1, 8, 12 and η Cha itself). Torres et al. considered η Cha to be a part of ϵ Cha and while the two groups have similar ages, distances and kinematics, in this work we consider only the 20 stars they classified as ϵ Cha ‘field members’. We will discuss the relationship between η and ϵ Cha in greater detail in §7.

Of the candidates not proposed as members by Torres et al. (2008), they rejected only three¹; RX J1150.4–7704 (ϵ Cha 19; Terranegra et al. 1999) had kinematics far from their convergent solution, HIP 55746 (Zuckerman & Song 2004) was reclassified as a member of the AB Doradus association and RX J1158.5–7754A (ϵ Cha 21; Terranegra et al. 1999) was a poor kinematic match at its 90 pc *Hipparcos* distance. The remaining stars lacked radial velocities necessary for the convergence method. Measuring velocities for these stars is one of the key contributions of this work.

2.2 New candidates

Several new ϵ Cha members have been proposed since the compilation of Torres et al. (2008). Kiss et al. (2011) suggested 2MASS J12210499–7116493 as a new member at an estimated kinematic distance of 98 pc. The star has strong Li I $\lambda 6708$ absorption and a velocity only 1.5 km s^{−1} from the Torres et al. space motion². Kastner et al. (2012) recently identified 2MASS J11550485–7919108 as a wide comoving companion to T Cha. It is spectroscopically young and hosts circumstellar material. Most recently, Lopez Martí et al. (2013) reanalysed the proper motions of young stars in Chamaeleon and proposed the new ϵ Cha member RX J1216.8–7753 as well as reclassifying the Cha II star CM Cha as a potential member of the association.

¹ Torres et al. did not test the membership of VW Cha, the only Frink et al. (1998) candidate not also included by Terranegra et al. (1999).

² Kiss et al. swapped the radial velocity of 2MASS J1221–71 with the β Pic member 2MASS J01071194–1935359 in their table 1. The listed space motions for both stars are consistent with their correct velocities.

Table 1. Proposed members of the ϵ Cha association from the literature

ID [§]	Name	Right Ascension [J2000]	Declination [J2000]	Spec. type [†]	V^{\dagger} [mag]	Membership* references	Torres et al. member?
	HD 82879	09 28 21.1	−78 15 35	F6	8.99	8	Y
	CP−68 1388	10 57 49.3	−69 14 00	K1	10.39	8	Y
	VW Cha	11 08 01.5	−77 42 29	K8	12.64	1	
	TYC 9414-191-1	11 16 29.0	−78 25 21	K5	10.95	3	
13	2MASS J11183572−7935548	11 18 35.7	−79 35 55	M4.5	14.91	7	
14	RX J1123.2−7924	11 22 55.6	−79 24 44	M1.5	13.71	7	
	HIP 55746	11 25 18.1	−84 57 16	F5	7.6	6	
15	2MASS J11334926−7618399	11 33 49.3	−76 18 40	M4.5	...	7	
	RX J1137.4−7648	11 37 31.3	−76 47 59	M2.2	...	6	
16	2MASS J11404967−7459394	11 40 49.7	−74 59 39	M5.5	17.28	7	
	TYC 9238-612-1	11 41 27.7	−73 47 03	G5	10.7	6	
17	2MASS J11432669−7804454	11 43 26.7	−78 04 45	M4.7	17.33	7	
	RX J1147.7−7842	11 47 48.1	−78 41 52	M3.5	...	6	
18	RX J1149.8−7850	11 49 31.9	−78 51 01	M0	12.9	7	Y
19	RX J1150.4−7704	11 50 28.3	−77 04 38	K4	12.0	1,2,6,7	
	RX J1150.9−7411 [‡]	11 50 45.2 [‡]	−74 11 13 [‡]	M3.7	14.4	2	
	2MASS J11550485−7919108	11 55 04.9	−79 19 11	M3	...	10	
	T Cha	11 57 13.5	−79 21 32	K0	12.0	1,2,6	Y
20	RX J1158.5−7754B	11 58 26.9	−77 54 45	M3	14.29	7	Y
21	RX J1158.5−7754A	11 58 28.1	−77 54 30	K4	10.9	1,2,3,6,7	
	HD 104036	11 58 35.4	−77 49 31	A7	6.73	3,6	Y
1	CXOU J115908.2−781232	11 59 08.0	−78 12 32	M4.75		4	
2	ϵ Cha AB	11 59 37.6	−78 13 19	B9	5.34	3,4	Y
	RX J1159.7−7601	11 59 42.3	−76 01 26	K4	11.31	1,2,3,6	Y
3	HD 104237C	12 00 03.6	−78 11 31	M/L	~25	4	
4	HD 104237B	12 00 04.0	−78 11 37	K/M	15.1	4	
5	HD 104237A	12 00 05.1	−78 11 35	A7.75	6.73	2,3,4	Y
6	HD 104237D	12 00 08.3	−78 11 40	M3.5	14.28	4	Y
7	HD 104237E	12 00 09.3	−78 11 42	K5.5	12.08	4	Y
10	2MASS J12005517−7820296	12 00 55.2	−78 20 30	M5.75	...	5	
	HD 104467	12 01 39.1	−78 59 17	G3	8.56	1,2,6	Y
11	2MASS J12014343−7835472	12 01 43.4	−78 35 47	M2.25	...	5	
8	USNO-B 120144.7−781926	12 01 44.4	−78 19 27	M5	...	4	
9	CXOU J120152.8−781840	12 01 52.5	−78 18 41	M4.75	...	4	
	RX J1202.1−7853	12 02 03.8	−78 53 01	M0	12.48	8	Y
	RX J1202.8−7718	12 02 54.6	−77 18 38	M3.5	14.4	2,6	
	RX J1204.6−7731	12 04 36.2	−77 31 35	M3	13.81	2,6	Y
	TYC 9420-676-1	12 04 57.4	−79 32 04	F0	10.28	3	
	HD 105234	12 07 05.5	−78 44 28	A9	7.4	3	
12	2MASS J12074597−7816064	12 07 46.0	−78 16 06	M3.75	...	5	
	RX J1207.7−7953	12 07 48.3	−79 52 42	M3.5	14.5	6	
	HIP 59243	12 09 07.8	−78 46 53	A6	6.9	6	
	HD 105923	12 11 38.1	−71 10 36	G8	9.16	8	Y
	RX J1216.8−7753	12 16 45.9	−77 53 33	M4	13.88	11	
	RX J1219.7−7403	12 19 43.5	−74 03 57	M0	13.08	2,6	Y
	RX J1220.4−7407	12 20 21.9	−74 07 39	M0	12.85	2,6	Y
	2MASS J12210499−7116493	12 21 05.0	−71 16 49	K7	12.16	9	
	RX J1239.4−7502	12 39 21.2	−75 02 39	K3	10.30	2,6	Y
	RX J1243.1−7458 [‡]	12 42 53.0 [‡]	−74 58 49 [‡]	M3.2	15.1	2	
	CD−69 1055	12 58 25.6	−70 28 49	K0	9.95	8	Y
	CM Cha	13 02 13.6	−76 37 58	K7	13.40	11	
	MP Mus	13 22 07.6	−69 38 12	K1	10.35	8	Y

(§) SIMBAD identifier [FLG2003] EPS CHA

(*) Membership references: (1) Frink et al. (1998), (2) Terranegra et al. (1999), (3) Mamajek et al. (2000), (4) Feigelson et al. (2003), (5) Luhman (2004b), (6) Zuckerman & Song (2004), (7) Luhman et al. (2008), (8) Torres et al. (2008), (9) Kiss et al. (2011), (10) Kastner et al. (2012), (11) Lopez Martí et al. (2013)

(‡) Updated coordinates to those presented by Alcalá et al. (1995). See Fig. A1.

(†) Spectral types from the literature (see Table B1) and our WiFeS observations. Indicative V magnitudes from SIMBAD.

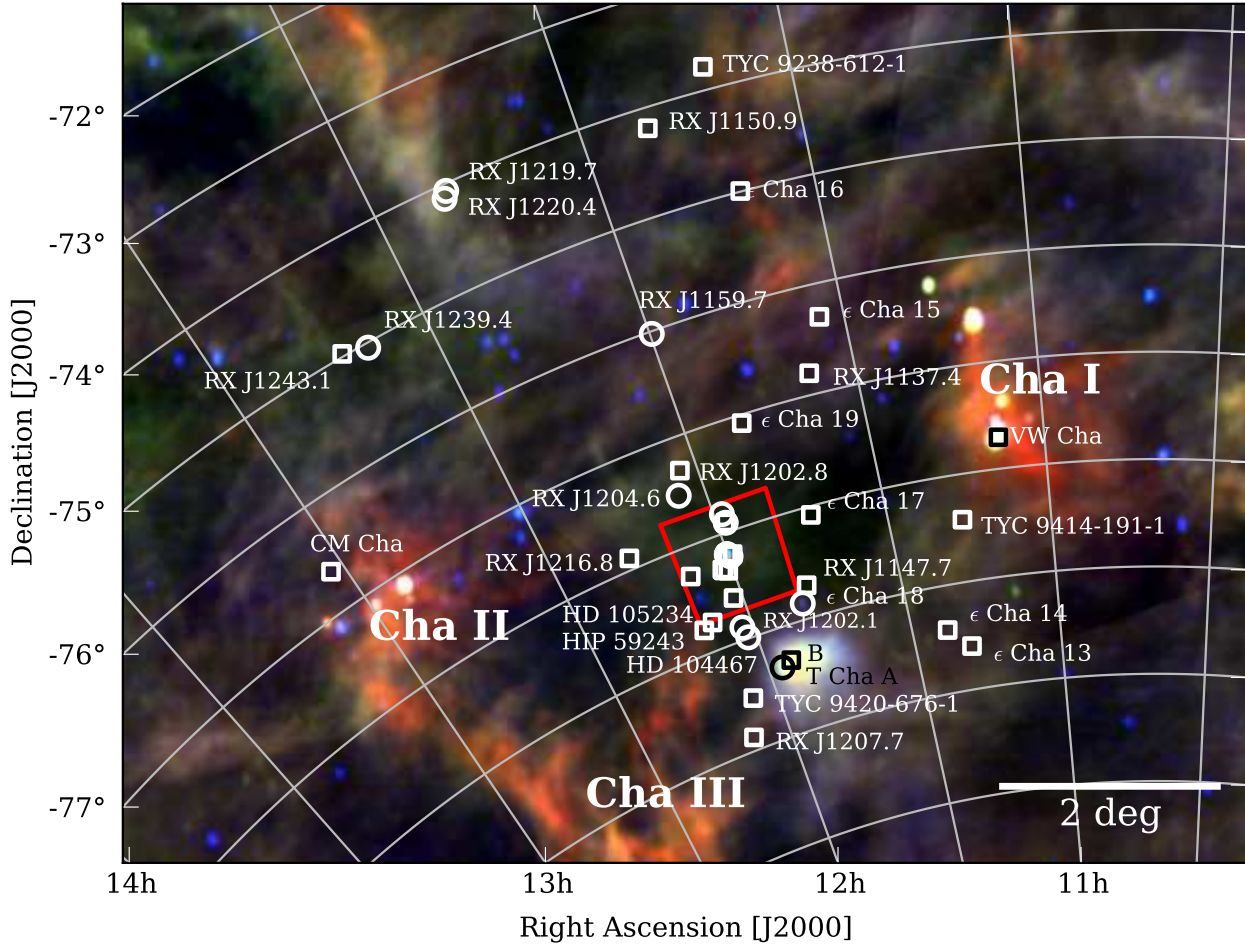


Figure 2. *Infrared Astronomical Satellite (IRAS)* 100/60/25 μm colour composite of the Chamaeleon region, with proposed ϵ Cha candidates from the literature (squares) and kinematic members from Torres et al. (2008) (circles). η Cha members in the Torres et al. solution, HD 82879, the likely AB Dor member HIP 55746 and several members north of $\delta = -72^\circ$ are not shown (see Fig. 22). The red square shows the 1 deg^2 extent of Fig. 1.

By tracing back in time the positions of nearby ($d < 30 \text{ pc}$) *Hipparcos* stars with radial velocities, Nakajima & Morino (2012) proposed an additional seven members of the ‘Cha-Near’ group of Zuckerman & Song (2004). Their proposed membership included the older pre-main sequence stars GJ 82 (estimated age 35–300 Myr; Shkolnik et al. 2009), DK Leo ($>400 \text{ Myr}$; Shkolnik et al. 2009), GJ 755 ($200 \pm 100 \text{ Myr}$; Barrado y Navascues 1998), HR 3499 ($>100 \text{ Myr}$; Wichmann et al. 2003), the β Pic member AF Lep (Torres et al. 2008) and the binary EQ Peg, whose M3.5 primary has only a marginal lithium detection (Zboril et al. 1997), implying an age greater than 10 Myr. The stars are highly unlikely to be ϵ Cha members and we discuss them no further.

Excluding the Nakajima & Morino candidates there are 52 putative members of the ‘ ϵ Cha association’ in the literature. They are listed in Table 1 with spectral types and membership references. Their astrometry has been resolved against Two Micron All Sky Survey (2MASS) images and our own spectroscopic observations (also see Appendix A). For candidates proposed by Feigelson et al. (2003), Luhman (2004b) and Luhman et al. (2008) we provide the ϵ Cha identification number (1–21) used in those studies. Figs. 1 and 2 show the location of ϵ Cha candidates on the sky. While the

region around ϵ Cha and HD 104237 (Fig. 1) is well-studied, the majority of the dispersed population are isolated *ROSAT* sources or incidental observations of stars around the Cha I cloud. Given the shallow depth of the flux-limited *ROSAT* All Sky Survey, future studies may reveal an extensive population of low-mass, X-ray-faint members across the region.

3 CANDIDATE OBSERVATIONS

3.1 Multi-epoch spectroscopy

Many of the proposed ϵ Cha members lack radial velocities necessary for confirming membership in a kinematic association. To remedy this and assess the youth of the candidates we observed 19 K and M-type stars from Table 1 with the Wide Field Spectrograph (WiFeS; Dopita et al. 2007) on the ANU 2.3-m telescope at Siding Spring. To constrain any velocity variations and investigate circumstellar accretion (Murphy et al. 2011), we observed each star 3–7 times over 60–480 d between 2010 February and 2011 June. We used the R7000 grating, which gave $\lambda/\Delta\lambda \approx 7000$ and coverage from 5300–7100 Å. Exposure times were 900–5400 s per epoch. To estimate spectral types, surface gravities and reddenings we also

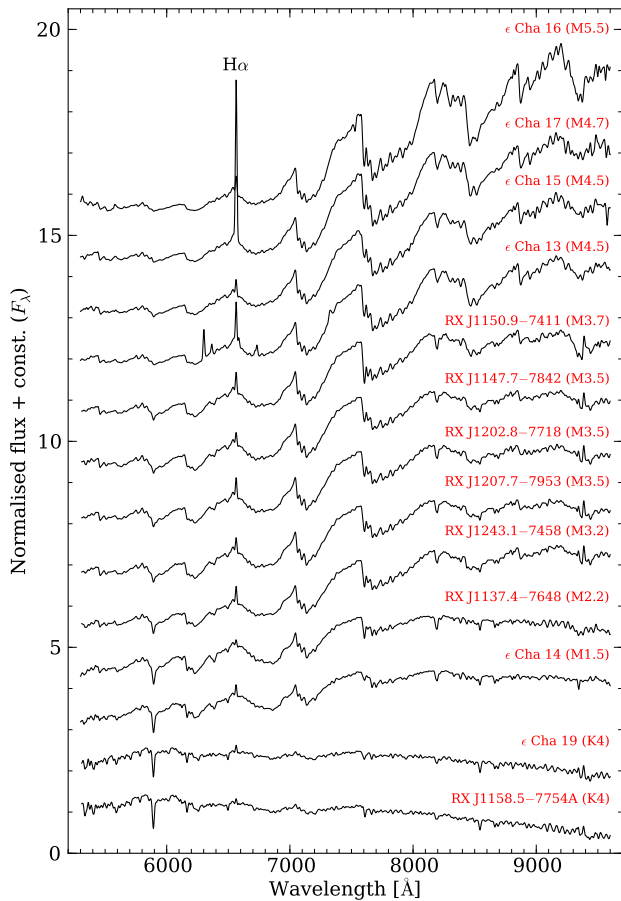


Figure 3. Flux-calibrated WiFeS/R3000 spectra of the low-mass candidates listed in Table 2. The spectra have been smoothed with a 10-px Gaussian kernel and normalised over the region 7400–7550 Å for display.

obtained single-epoch $R3000$ spectra (5300–9600 Å) for ϵ Cha 13–17 and several *ROSAT* candidates during 2011 July 30–31. All the spectra were observed and reduced as described in Murphy et al. (2010, 2012). Radial velocities at each epoch were calculated by cross-correlation of the $R7000$ spectra against 5–7 K and M-type standards observed that night.

The WiFeS/ $R3000$ spectra are plotted in Fig. 3. RX J1137.4–7648 and RX J1147.7–7842 (Zuckerman & Song 2004) have no previously published spectroscopy. The former is a 3 arcsec approximately equal-brightness visual binary that was unresolved in the typical 2–2.5 arcsec seeing of the $R3000$ observations. During a night of exceptional $\lesssim 1$ arcsec seeing on 2011 May 16 we resolved the pair and extracted minimally-blended $R7000$ spectra. A full listing of WiFeS spectral types, Li I $\lambda 6708$ and $H\alpha$ equivalent widths and mean radial velocities are given in Table 2. Fifteen candidates have no previous velocity measurement.

3.2 Spectral types and reddening

We determined the spectral types in Table 2 using a selection of molecular indices from the list of Riddick et al. (2007) and comparison to η and ϵ Cha spectra from Lyo et al. (2004a, 2008). We used the grid of Pickles (1998) to extend our classification to K and early-M spectral types. The WiFeS/ $R3000$ values agree with those previously determined at the 0.2–0.3 subtype level.

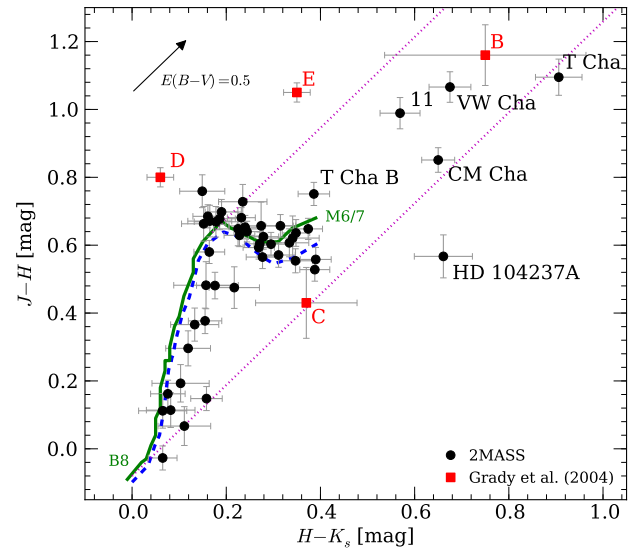


Figure 4. 2MASS two-colour diagram for ϵ Cha candidates (small points), with photometry for HD 104237B–E from Grady et al. (2004) (red squares). The main sequence intrinsic colours of Kraus & Hillenbrand (2007, solid line) and Bessell & Brett (1988, dashed line) and reddening vector of Schlegel et al. (1998, dotted lines) have been transformed to the 2MASS system using the relations of Carpenter (2001).

With the exception of VW Cha (which appears associated with Cha I) and T Cha AB (possibly associated with the dark cloud Dcd 300.2–16.9) the proposed members are spread between the Chamaeleon clouds in a region of low-intensity dust emission (see Fig. 2). This is also apparent in the 2MASS two-colour diagram of Fig. 4, where the majority of candidates closely follow the expected zero-reddening locus. However, the region is filled with dozens of small, isolated molecular cloudlets (Knee & Prusti 1996; Mizuno et al. 1998) and there is evidence of foreground reddening between the Sun and the cloud complex (Knude & Hog 1998). Compared to (unreddened) η Cha spectra we estimate 2MASS J11334926–7618399 (ϵ Cha 15) is reddened by approximately $E(B - V) \approx 0.15$ mag, while 2MASS J11432669–7804454 (ϵ Cha 17) and RX J1243.1–7458 are both reddened by no more than 0.1 mag. To supplement the WiFeS candidates we estimated reddenings for all the candidates using Fig. 4 as well as literature spectral types and photometry. The results and adopted spectral types are listed in Table B1.

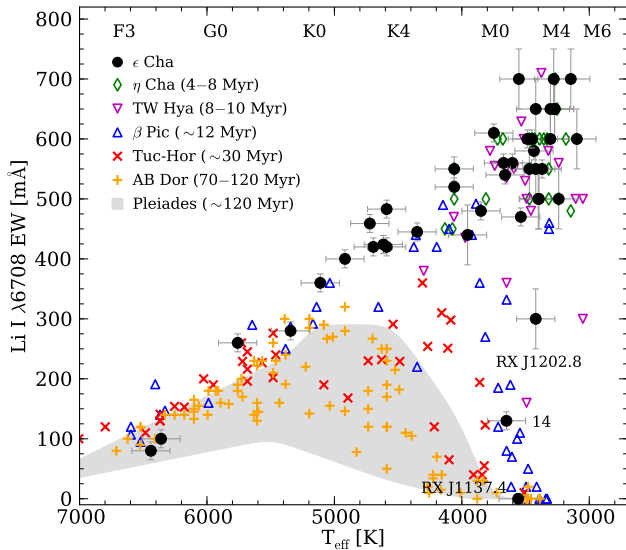
3.3 Lithium depletion

The amount of photospheric lithium depletion observed in low-mass stars can serve as a mass-dependent clock over pre-main sequence time-scales (e.g. Mentuch et al. 2008; da Silva et al. 2009). We plot in Fig. 5 the distribution of candidate Li I $\lambda 6708$ equivalent widths assembled from the literature and our WiFeS observations. The individual measurements and their sources are listed in Table B1. Seven stars have no lithium information. Two of these are A-type stars (HD 105234, HIP 59243) and are not expected to show lithium absorption. The remaining five stars (HD 104237B/C, TYC 9414-191-1, TYC 9238-612-1, and TYC 9420-676-1) do not have any available spectroscopy.

We also plot in Fig. 5 the lithium data for confirmed members of young associations from da Silva et al. (2009). The sensitivity of lithium depletion to both stellar age and mass is evident in the older

Table 2. WiFeS observations of ϵ Cha candidates from the literature

ID	Name	Spec. [†] type	$E(B - V)^{\dagger}$ [mag]	Li I EW [± 50 mÅ]	RV [km s ⁻¹]	σ_{RV}^{\ddagger} [km s ⁻¹]	H α EW [± 1 Å]	N_{obs}	Δt [days]
13	2MASS J11183572–7935548	M4.5	0	600	19.3*	1.6*	[–30, –18]	7	477
14	RX J1123.2–7924	M1.5	0	150	2.7*	2.9*	–2	6	477
15	2MASS J11334926–7618399	M4.5	0.15	650	16.7*	1.5*	–6	5	413
	RX J1137.4–7648	M2.2	0	0	~14	...	–1.5	1	...
16	2MASS J11404967–7459394	M5.5	0	700	10.3	1.0	[–35, –11]	4	411
17	2MASS J11432669–7804454	M4.7	<0.1	700	15.6	1.0	[–120, –60]	6	480
	RX J1147.7–7842	M3.5	0	650	16.1	0.9	[–7, –4]	5	409
19	RX J1150.4–7704	K4	0	500	6.1*	1.6*	–1	5	479
	RX J1150.9–7411	M3.7	0	500	15.0	1.2	–8	4	59
21	RX J1158.5–7754A	K4	0	500	19.9	0.8	–0.5	4	480
1	CXOU J115908.2–781232	650	15.1	0.2	–5	3	356
10	2MASS J12005517–7820296	600	10.7*	1.3*	[–20, –10]	6	411
11	2MASS J12014343–7835472	700	20.0	0.6	[–140, –70]	3	370
8	USNO-B 120144.7–781926	500	14.9	1.1	[–45, –20]	4	60
9	CXOU J120152.8–781840	650	16.5	1.1	–8	4	411
	RX J1202.8–7718	M3.5	0	300	17.1	1.2	[–12, –5]	4	411
12	2MASS J12074597–7816064	500	15.4*	2.3*	–3.5	5	410
	RX J1207.7–7953	M3.5	0	550	15.0	0.7	–4	4	414
	RX J1243.1–7458	M3.2	<0.1	600	13.5	0.7	[–7, –4]	4	60

(†) Spectral types and reddening values determined from WiFeS $R3000$ spectra(★) WiFeS $R7000$ time series shows a velocity trend indicative of binarity (see §4.2.1 and Table 5)(‡) Standard error of the mean, $\sigma_{RV} = \sigma / \sqrt{N_{\text{obs}}}$ **Figure 5.** Li $\lambda 6708$ equivalent widths for ϵ Cha candidates (black points, with errors), compared to members of young, nearby associations from da Silva et al. (2009). Members of the η Cha open cluster and the envelope of equivalent widths observed in the Pleiades are also plotted. Following da Silva et al., effective temperatures were calculated from the spectral-type T_{eff} relation of Kenyon & Hartmann (1995).

associations. By an age of 8–10 Myr, several late-type members of the TW Hydrae association have already begun to show significant depletion and the slightly older β Pictoris association (~ 12 Myr) presents a steep decline in equivalent widths down to its lithium depletion boundary at a spectral type of $\sim M4$. The vast majority of late-type ϵ Cha candidates have Li I $\lambda 6708$ equivalent widths consistent with an age no older than the 4–8 Myr η Cha cluster. Three

candidates have lithium measurements inconsistent with such a young age; RX J1202.8–7718, RX J1123.2–7924 (ϵ Cha 14) and RX J1137.4–7648. The non-detection of lithium in the latter implies it is at least as old as members of the Tucana-Horologium association (~ 30 Myr). The system’s inclusion in Cha-Near by Zuckerman & Song (2004) was also inconsistent with lithium measurements taken at the time by the same authors (private communication). The two other stars have levels of lithium depletion similar to members of TW Hya or β Pic (age ~ 8 –12 Myr).

4 KINEMATIC MEMBERSHIP ANALYSIS

4.1 Proper motions

To derive a kinematic solution for ϵ Cha and test the membership of each candidate it is necessary to obtain the best-possible proper motions and radial velocities. Nine candidates have proper motions in the latest reduction of the *Hipparcos* catalogue (van Leeuwen 2007) and a further ten were recovered in Tycho-2 (Høg et al. 2000). We adopted these proper motions in our analysis with the exception of T Cha, which has a large error in *Hipparcos* and is not found in Tycho-2. For this star we used the higher-precision value from SPM4, the fourth iteration of Yale/San Juan Southern Proper Motion Catalog (Girard et al. 2011). SPM4 contains absolute proper motions for over 103 million stars and galaxies, including nearly all of the proposed ϵ Cha members. Only HD 104237B/C and 2MASS J12014343–7835472 (underluminous due to an edge-on disk; Luhman 2004b) were not found in SPM4. We also cross-matched the candidate list against the recent UCAC4 (Zacharias et al. 2013) and PPMXL (Röser et al. 2010) proper motion catalogues, but these gave fewer matches and in the case of PPMXL much less precise astrometry (also see discussion in Girard et al. 2011).

The results of these cross-matches are summarised in Fig. 6.

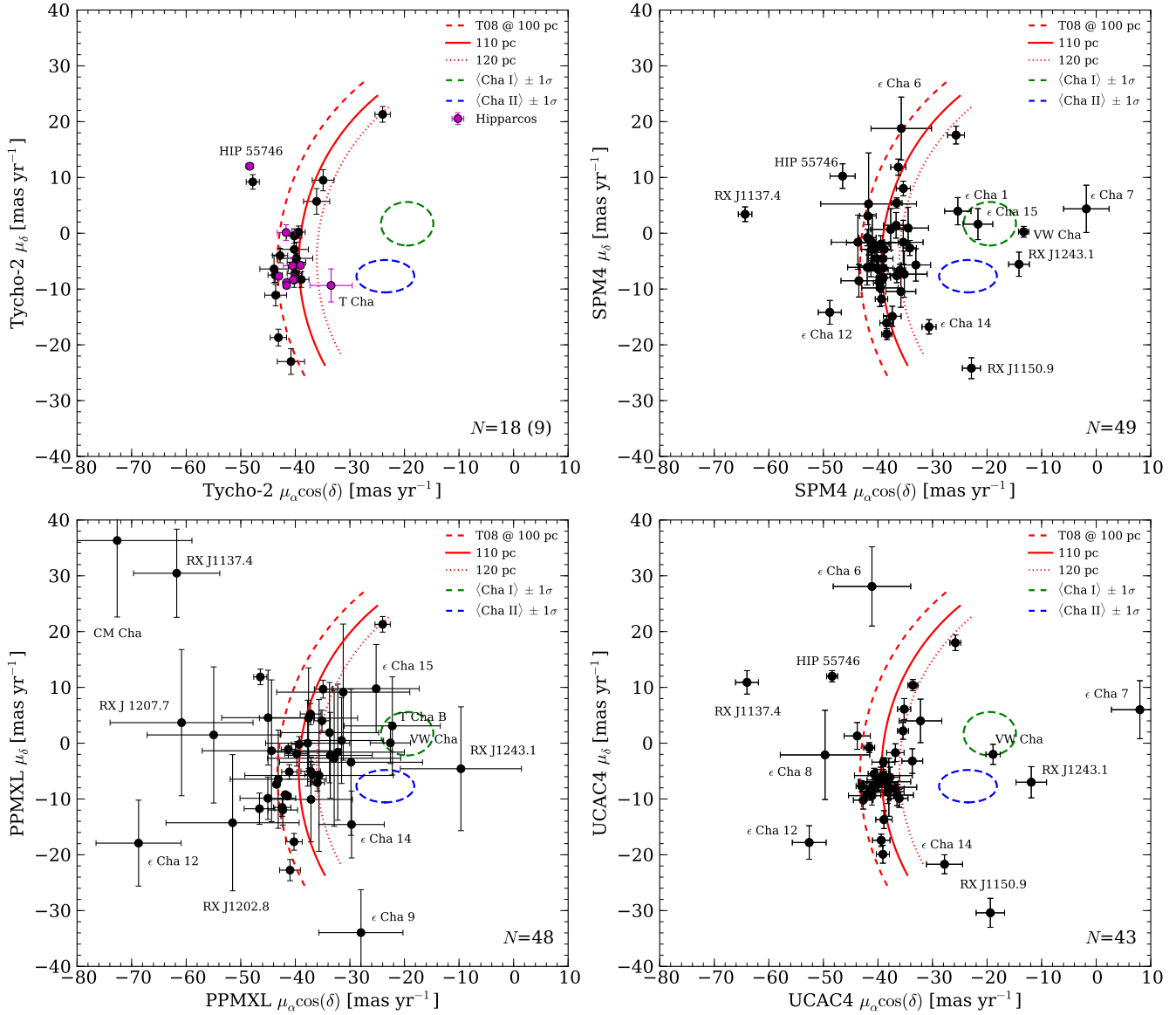


Figure 6. Proper motions of candidates in the *Hipparcos*/Tycho-2 (top left), SPM4 (top right), PPMXL (bottom left) and UCAC4 (bottom right) catalogues. The number of matches is given in the corner of each panel. The red lines show the Torres et al. (2008) space motion projected onto the sky at $\delta = -79^\circ$ and $130^\circ < \alpha < 210^\circ$ and distances of 100–120 pc. Green and blue ellipses are the mean proper motions of Cha I and II from Lopez Martí et al. (2013).

SPM4 and UCAC4 are somewhat correlated as they share some first epoch astrophotograph data (Zacharias et al. 2013). As expected, the majority of stars cluster around the projection of the ϵ Cha space motion on the sky at 100–120 pc. However, there are several candidates with proper motions far from those expected of members.

4.1.1 Outlying proper motions

HIP 55746 was reclassified as a member of the AB Doradus association by Torres et al. (2008); its *Hipparcos* proper motion and parallax are consistent with this new classification. RX J1137.4–7648 is likely a nearby older system. Its astrometry may also have been affected by orbital motion. CXOU J120152.8–781840 (ϵ Cha 9) and 2MASS J12074597–7816064 (ϵ Cha 12) were noted by Fang et al. (2013) as having outlying PPMXL proper motions. With the new UCAC4 and SPM4 astrometry only ϵ Cha 12 remains an

outlier. As it has a spectroscopic age consistent with other proposed members its status is unclear. RX J1123.2–7924 (ϵ Cha 14) also has a slightly discrepant proper motion, though its level of lithium depletion implies an age older than ϵ Cha. Terranegra et al. (1999) found RX J1243.1–7458 was a kinematic but not spatial outlier to their proposed moving group. Its proper motion is near the mean of Cha II cloud members (Lopez Martí et al. 2013). VW Cha, CXOU J115908.2–781232 (ϵ Cha 1) and 2MASS J11334926–7618399 (ϵ Cha 15) may similarly be associated with Cha I. HD 104237D and E (ϵ Cha 6 and 7) are probably affected by their location close to HD 104237A. RX J1150.9–7411 has a close companion (Köhler 2001) which may have altered the motion of its photo-centre.

Table 3. Candidates whose SPM4 and UCAC4 proper motions disagree by more than 2σ

Name	SPM4 [mas yr ⁻¹]		UCAC4 [mas yr ⁻¹]		PPMXL [mas yr ⁻¹]	
	$\mu_\alpha \cos \delta$	μ_δ	$\mu_\alpha \cos \delta$	μ_δ	$\mu_\alpha \cos \delta$	μ_δ
VW Cha	-13.3 ± 0.9	$+0.3 \pm 1.0$	-18.9 ± 1.3	-2.0 ± 1.8	-22.6 ± 3.7	$+0.1 \pm 3.7$
RX J1123.2–7924 (ϵ Cha 14)	-30.6 ± 1.3	-16.8 ± 1.3	-27.8 ± 3.3	-21.7 ± 1.7	-29.7 ± 6.0	-14.6 ± 6.0
RX J1137.4–7648	-64.4 ± 1.2	$+3.4 \pm 1.3$	-64.0 ± 2.1	$+10.9 \pm 2.1$	-61.7 ± 7.9	$+30.5 \pm 7.9$
CM Cha	-33.1 ± 2.7	-5.7 ± 2.9	-32.2 ± 3.9	$+4.0 \pm 3.9$	-72.7 ± 13.7	$+36.3 \pm 13.7$

Table 4. Candidates whose Ducourant et al. (2005) or Terranegra et al. (1999) proper motions disagree with SPM4 by more than 2σ

Name	SPM4 [mas yr ⁻¹]		Ducourant et al. (2005) [mas yr ⁻¹]		Terranegra et al. (1999) [mas yr ⁻¹]	
	$\mu_\alpha \cos \delta$	μ_δ	$\mu_\alpha \cos \delta$	μ_δ	$\mu_\alpha \cos \delta$	μ_δ
VW Cha	-13.3 ± 0.9	$+0.3 \pm 1.0$	-24 ± 3	$+2 \pm 3$
RX J1150.9–7411	-22.9 ± 1.7	-24.2 ± 1.9	$+15 \pm 16$	$+37 \pm 16$	-39.0 ± 4.2	$+4.4 \pm 2.9$
RXJ1219.7–7403	-39.0 ± 1.3	-8.0 ± 1.5	-37 ± 11	-15 ± 11	-40.4 ± 6.9	-2.8 ± 0.2
CM Cha	-33.1 ± 2.7	-5.7 ± 2.9	-66 ± 12	$+23 \pm 12$

4.1.2 Discordant proper motions

After comparing SPM4 and UCAC4 there were four stars with proper motions that differed by more than 2σ in either component. Their astrometry is collated in Table 3, with values from PPMXL for comparison. Terranegra et al. (1999) and Ducourant et al. (2005) calculated proper motions for 15 and 20 of the candidates, respectively. Because of their different source observations these studies provide an independent check on the SPM4 measurements. The four stars whose proper motions disagreed with SPM4 by more than 2σ are listed in Table 4.

The Ducourant et al. proper motion for VW Cha agrees with both UCAC4 and PPMXL. We adopted the UCAC4 value, while for RX J1123.2–7924 (ϵ Cha 14) and RX J1137.4–7648 we retained the SPM4 proper motions. CM Cha is a special case. Although the Ducourant et al. proper motion matches PPMXL within the (large) errors we have adopted the higher-precision SPM4 values. If the larger proper motion is correct then CM Cha may be even closer to the Sun than ϵ Cha (see discussion in Lopez Martí et al. 2013). The motion of RX J1150.9–7411 measured by both studies differs significantly from SPM4 and UCAC4. While Ducourant et al. used an incorrect position from Alcalá et al. (1995) and gave the proper motion of an unrelated star (see Appendix A), the Terranegra et al. proper motion for RX J1150.9–7411 is very close to other ϵ Cha candidates. We chose this value over SPM4 but note that it may also be influenced by the star’s close companion (Köhler 2001). Finally, the error in the μ_δ component of RXJ1219.7–7403 calculated by Terranegra et al. is likely underestimated and we adopted the SPM4 measurement. The proper motions of all candidates and their sources are listed in Table B1.

4.2 Radial velocities

To supplement the WiFeS measurements we searched the literature for candidate radial velocities. These are also listed in Table B1. HD 104237B/C, the three Tycho stars, HD 105234 and HIP 59243 have no published velocities. For 2MASS J11550485–7919108 (T Cha B) we adopted the value for T Cha itself, 14.0 ± 1.3 km s⁻¹ (Guenther et al. 2007). Since T Cha exhibits large ($\Delta RV \sim 10$ km s⁻¹) aperiodic velocity variations on daily time-scales (Schisano et al. 2009) we caution that this velocity may not be

representative. However, it agrees with velocities reported by Torres et al. (2006) (16.3 ± 5.8 km s⁻¹) and Franchini et al. (1992) (14.6 ± 2.1 km s⁻¹). For HD 104237E we adopted the velocity of the D component, 13.4 km s⁻¹ (Grady et al. 2004). The authors of that study stated that both stars were a good velocity match to HD 104237A (14 km s⁻¹), although they did not explicitly give a velocity for the E component.

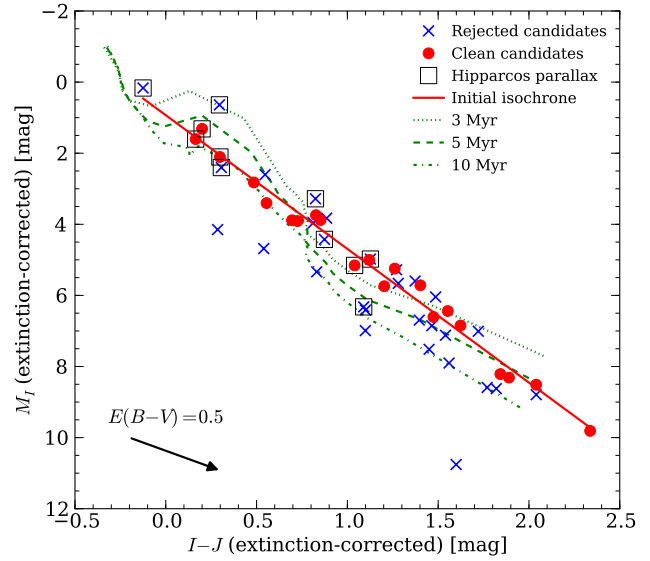
4.2.1 Spectroscopic binaries

The multi-epoch WiFeS observations revealed six candidates (marked in Table 2) with velocity variations indicative of binarity. Two more candidates, RX J1158.5–7754A (ϵ Cha 21) and RX J1243.1–7458, have mean velocities that differ significantly from those in the literature. The velocities of these eight stars are presented in Table 5. The individual errors in this table are the standard deviations of cross-correlations against 4–8 K and M-type standards observed each night. We also found that the Torres et al. (2008) members RX J1202.1–7853 and RX J1220.4–7407 have velocities in Guenther et al. (2007) and Covino et al. (1997) that differ outside their errors. These stars are also listed in Table 5.

Köhler (2001) conducted a speckle and direct-imaging survey for close (0.13–6 arcsec) companions around 82 *ROSAT* sources in Chamaeleon, including six of the candidates in Table 5. We have confirmed the binarity of RX J1158.5–7754A (ϵ Cha 21), RX J1243.1–7458 and RX J1220.4–7407. Köhler (2001) also found close companions around HIP 55746 (probable AB Dor member) and RX J1150.9–7411. Four WiFeS measurements of the latter over 59 d showed no significant velocity variation, unsurprising given the cadence of the observations. Despite Köhler finding no companions around RX J1123.2–7924 (ϵ Cha 14) the star is clearly a spectroscopic binary. We have also confirmed suspicions about the binarity of RX J1150.4–7704 (ϵ Cha 19) raised by Covino et al. (1997), with both our WiFeS time-series and an earlier measurement by Guenther et al. (2007) showing a clear velocity variation. With only two measurements we cannot confirm the spectroscopic binarity of RX J1202.1–7853, though the large velocity difference (12.1 ± 2 km s⁻¹) is compelling.

Table 5. Candidates suspected of spectroscopic binarity

Star Epoch	RV [km s ^{−1}]	σ(RV) [km s ^{−1}]	Köhler (2001) companion?
2MASS J12005517−7820296 (ϵ Cha 10)			...
2010 May 04	+15.0	1.1	
2011 Jan 09	+7.2	0.8	
2011 Feb 24	+9.0	2.0	
2011 May 09	+13.4	1.1	
2011 May 17	+12.0	1.7	
2011 Jun 19	+7.5	1.0	
2MASS J12074597−7816064 (ϵ Cha 12)			...
2010 May 05	+23.4	1.5	
2011 Jan 08	+10.7	0.8	
2011 Jan 13	+15.2	1.9	
2011 May 17	+16.7	1.1	
2011 Jun 19	+11.0	0.5	
2MASS J11183572−7935548 (ϵ Cha 13)			...
2010 Feb 25	+19.8	2.6	
2010 May 02	+15.8	0.5	
2010 Dec 20	+14.3	1.9	
2011 Feb 11	+17.9	1.2	
2011 Feb 12	+17.8	2.5	
2011 May 16	+26.7	1.2	
2011 Jun 17	+23.2	2.7	
RX J1123.2−7924 (ϵ Cha 14)			N (#42)
2010 Feb 25	−2.6	3.1	
2010 May 02	−5.0	0.1	
2010 Dec 20	−0.4	1.7	
2011 Feb 10	+2.4	0.4	
2011 May 16	+7.3	1.8	
2011 Jun 17	+14.1	2.1	
Covino et al. (1997)	+10.0	2.0	
2MASS J11334926−7618399 (ϵ Cha 15)			...
2010 May 02	+13.9	0.6	
2010 Dec 20	+14.0	1.5	
2011 Feb 11	+15.1	0.7	
2011 May 16	+20.4	1.5	
2011 Jun 19	+20.1	0.6	
RX J1150.4−7704 (ϵ Cha 19)			N (#47)
2010 Feb 25	+9.0	3.5	
2010 May 06	+9.7	1.7	
2011 Feb 10	+6.2	0.4	
2011 May 17	+1.0	1.7	
2011 Jun 19	+4.5	1.4	
Covino et al. (1997)	SB?		
Guenther et al. (2007)	−3.3	1.0	
RX J1158.5−7754A (ϵ Cha 21)			Y (#50, 0.07'')
2010 Feb−2011 Jun	+19.9	0.8	
Covino et al. (1997)	+13.1	2.0	
James et al. (2006)	+10.2	...	
RX J1243.1−7458			Y (#73, 0.3'')
2011 Apr−Jun	+13.5	0.7	
Covino et al. (1997)	+7.0	2.0	
RX J1202.1−7853			N (#55)
Guenther et al. (2007)	+17.1	0.2	
Covino et al. (1997)	+5	2	
RX J1220.4−7407			Y (#65, 0.3'')
Guenther et al. (2007)	+12.3	0.4	
Covino et al. (1997)	+18	2	

**Figure 7.** The initial isochrone (solid line) used in the kinematic analysis. A linear fit was performed on the extinction-corrected photometry (red circles) after excluding binaries, proper motion and Li I outliers and NIR excess sources (blue crosses). Siess et al. (2000) theoretical isochrones (green lines) are shown for comparison.

4.2.2 Other known or suspected binaries

RX J1204.6–7731 is a double-lined spectroscopic binary (Torres et al. 2008) and HD 104467 is a suspected single-line system (Cutispoto et al. 2002). RX J1137.4–7648 and ϵ Cha are approximately equal-brightness visual binaries and VW Cha is a hierarchical triple (Correia et al. 2006). Böhm et al. (2004) detected a $1.7 M_{\odot}$ \sim K3 companion to HD 104237A in an eccentric 19.8 d orbit (separation \sim 0.1 au) which they called HD 104237b. It is likely the source of the late-type spectral features in HD 104237A reported by Feigelson et al. (2003) and is distinct from HD 104237B, which is resolved at \sim 150 au (1.3 arcsec).

4.3 Initial observational isochrone

To calculate photometric distances to the candidates an absolute magnitude is required. We plot in Fig. 7 the extinction-corrected photometry of ϵ Cha candidates with pre-main sequence isochrones from Siess et al. (2000) for comparison. Candidates without *Hipparcos* parallaxes were assigned a distance of 110 pc and we adopted the reddening relations $A_I = 0.601A_V$ and $A_{I-J} = 0.325A_V$ from Schlegel et al. (1998). Rather than use a theoretical isochrone, which would give inconsistent distances across the full colour (mass) range, we adopted a similar strategy to Torres et al. (2006) and used the candidates themselves to define an ad hoc isochrone. After excluding known or suspected binaries, proper motion outliers and those stars with 2MASS colour excesses or low Li I λ 6708 equivalent widths, the 21 remaining candidates were well-fitted by the linear regression:

$$M_I = 3.760 \times (I - J) + 0.93 \quad (1)$$

This relation was used in the kinematic analysis in the next section. As noted by Torres et al. (2006), defining an isochrone assuming membership in a group then using it to test membership appears to be circular reasoning. However, the high-quality candidates used to define Eqn. 1 all have photometry, proper motions,

radial velocities and lithium measurements consistent with membership in ϵ Cha and are highly likely to represent the true association isochrone. Moreover, several stars have *Hipparcos* parallaxes which anchor the distance scale of the fainter candidates.

Although binaries were not included in the calculation of Eqn. 1, before running the kinematic analysis we corrected the photometry of RX J1150.9–7411, RX J1158.5–7754A (ϵ Cha 21), RX J1220.4–7407, RX J1243.1–7458, HIP 55746, ϵ Cha and VW Cha to that of the primary using published flux ratios. For RX J1137.4–7648 we assumed an equal-mass system. More details and *IJKs* photometry for all candidates is given in Table B2.

4.4 Kinematic membership analysis

With the best-available proper motions, velocities and photometry we tested membership of the candidates using a similar technique to the ‘convergence’ method of Torres et al. (2006, 2008). For each star without a good *Hipparcos* parallax³ we first found the distance which minimised the difference in space motions:

$$K = \sqrt{(U - U_0)^2 + (V - V_0)^2 + (W - W_0)^2} \quad (2)$$

where $K = K(\alpha, \delta, \mu_\alpha, \mu_\delta, RV; d)$ and (U_0, V_0, W_0) is the mean space motion (from Torres et al. 2008)⁴. With this kinematic distance (or a parallax) and the extinction-corrected photometry we then calculated the difference in absolute magnitude (ΔM_I) between the candidate and the isochrone (Eqn. 1). Stars were retained as possible members if $K < 3.5 \text{ km s}^{-1}$ (a difference of $\sim 2 \text{ km s}^{-1}$ in each direction) and $|\Delta M_I| < 1 \text{ mag}$. To exclude background members of Cha I and II we additionally required $d < 150 \text{ pc}$. From these kinematic members a new isochrone and (U_0, V_0, W_0) was calculated. The process was iterated until the membership list and space motion no longer changed significantly.

5 RESULTS

Due to the high-quality initial space motion from Torres et al. (2008) the final list of 25 kinematic members converged on the second iteration while final distances and velocities took four iterations (for $\Delta d = 1 \text{ pc}$). Both the mean space motion (Table 6) and distance ($110 \pm 7 \text{ pc}$) agree with those previously determined by Torres et al. (2008). The revised values should be more accurate as they were derived from a larger number of members and by not subsuming η Cha into the ϵ Cha solution.

Fig. 8 summarises the convergent solution and Fig. 9 shows the final distribution of K and ΔM_I values. There are several candidates with $|\Delta M_I| < 1 \text{ mag}$ but velocity differences in excess of the 3.5 km s^{-1} limit. To account for non-systemic radial velocities and the lower-resolution WiFeS observations we selected as *a posteriori* kinematic members those candidates with $K < 8 \text{ km s}^{-1}$. Six of the eight stars this criteria added are known or suspected spectroscopic binaries. The mean space motion and isochrone were *not* updated after this step. The three rejected candidates inside the shaded selection box are CXOU J115908.2–781232 (ϵ Cha 1), 2MASS J11334926–7618399 (ϵ Cha 15) and RX J1243.1–7458. These stars have kinematic distances greater than 150 pc. Fig. 10

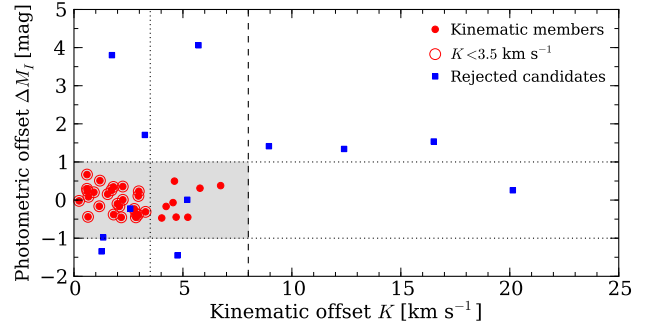


Figure 9. Results of the convergent analysis, showing the difference in space motions (K) and the offset from the final isochrone (ΔM_I). Dotted lines mark the $\pm 1 \text{ mag}$ and 3.5 km s^{-1} limits for calculating the association space motion (open circles), while the dashed line is the limit for selecting final kinematic members (filled circles).

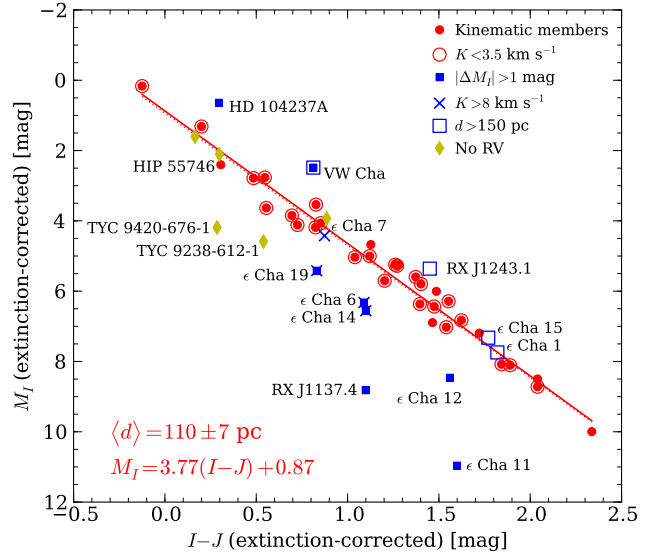


Figure 10. CMD of ϵ Cha from the kinematic analysis. Candidates rejected in the analysis (blue squares, crosses) are labelled. HD 104237A, ϵ Cha 6, 7 and 11 are confirmed members (see text). The five stars without radial velocities (yellow diamonds) are plotted at their best-fitting kinematic distance or *Hipparcos* parallax if available.

presents the association colour-magnitude diagram (CMD) and the twelve candidates rejected by the convergence technique. The tight grouping of kinematic members along the isochrone suggests the majority are true members of ϵ Cha.

Kinematic distances for the candidates observed by *Hipparcos* are compared with their trigonometric parallaxes in Fig. 11. In all cases the two distances agree within the 2σ parallax errors. Only two *Hipparcos* distances (ϵ Cha, HD 104036) were used in the final space motion solution. The other candidates had large parallax errors or failed one of the convergence criteria. For these stars we adopted the kinematic distances.

5.1 Notes on individual candidates

5.1.1 Confirmed members

CXOU J120152.8–781840 (ϵ Cha 9): Fang et al. (2013) questioned membership of this star based on its PPMXL proper motion.

³ For *Hipparcos* candidates with a parallax error greater than 10 per cent we adopted the kinematic distance.

⁴ Throughout this work (U, V, W) are a right-handed triad with U (and X) increasing towards the Galactic centre.

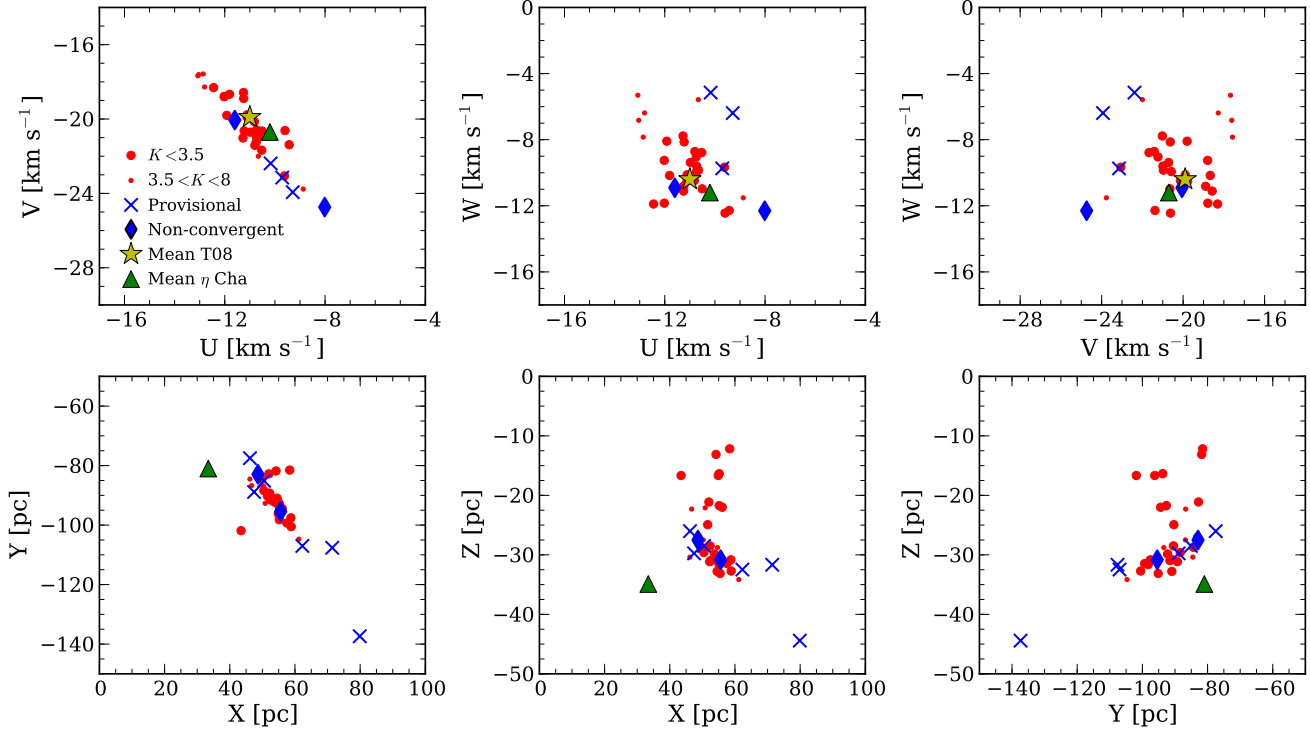


Figure 8. Heliocentric velocities and positions of kinematic members (red points), confirmed members not selected by the convergent analysis (HD 104237 and ϵ Cha 11; blue diamonds) and provisional candidates requiring confirmation (crosses). ϵ Cha 1 is shown at the 165 pc distance implied by its SPM4 proper motion. The previous Torres et al. (2008) and updated η Cha space motions are given by the yellow star and green triangle, respectively.

Table 6. Heliocentric velocities and positions of η and ϵ Chamaeleontis.

...	U	σ_U	V	σ_V	W	σ_W	X	σ_X	Y	σ_Y	Z	σ_Z
	[km s ⁻¹]						[pc]					
ϵ Cha (this work)	-10.9	0.8	-20.4	1.3	-9.9	1.4	54	3	-92	6	-26	7
Torres et al. (2008)	-11.0	1.2	-19.9	1.2	-10.4	1.6	50	...	-92	...	-28	...
η Cha (updated) [‡]	-10.2	0.2	-20.7	0.1	-11.2	0.1	33.4	0.4	-81.0	1.0	-34.9	0.4

([‡]) Derived from the weighted mean *Hipparcos*/Tycho-2 positions and proper motions of η Cha, RS Cha, RECX 1 and HD 75505 (08^h40^m48.24^s, -79° 00' 24.8"; $\mu_{\alpha} \cos \delta = -29.35 \pm 0.13$ mas yr⁻¹, $\mu_{\delta} = 27.41 \pm 0.13$ mas yr⁻¹), the weighted mean *Hipparcos* parallaxes of η Cha and RS Cha (94.3 ± 1.1 pc; van Leeuwen 2007) and the weighted mean radial velocities of RECX 1,3,4-6,9,10-13 (18.3 ± 0.1 km s⁻¹; A. Brandeker, unpublished private communication).

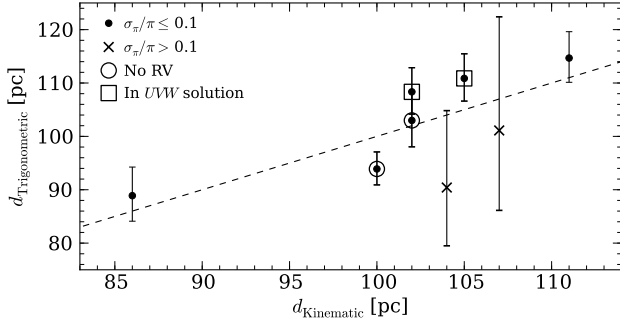


Figure 11. Comparison of trigonometric and kinematic distances. Kinematic distances for those stars without radial velocities were estimated from proper motions alone. The dashed line is the 1:1 relation. T Cha (relative parallax error ~ 50 per cent) is not plotted.

It was not recovered in UCAC4 but using higher-precision SPM4 astrometry we find it is a kinematic member at 121 pc.

RX J1149.8-7850 (ϵ Cha 18): Malo et al. (2013) assigned the star to β Pic. Their Bayesian analysis (which did not include ϵ Cha) gave a distance of 71 pc, which would make it one of the most distant members. Given its large Li I $\lambda 6708$ equivalent width (560 mÅ), it is likely younger than β Pic and we find an excellent match to ϵ Cha at a distance of 110 pc.

RX J1150.9-7411: Using the Terranegra et al. (1999) proper motion (see §4.1.2) we find RX J1150.9-7411 to be a kinematic member at 108 pc with $K = 4.6$ km s⁻¹ and $\Delta M_I = 0.5$ mag. The star has a close companion (Köhler 2001) and we caution that the WiFeS velocity may not be systemic.

RX J1158.5-7754AB (ϵ Cha 21+20): The 104 pc kinematic distance adopted for RX J1158.5-7754A barely agrees with its *Hipparcos* parallax (90.4⁺¹⁴₋₁₁ pc). Köhler (2001) detected a 0.07 arcsec companion and the system is only 16 arcsec from ϵ Cha 20

Table 7. Confirmed members of the ϵ Cha association

ID	Name	Spec. Type	Dist.* [pc]	K^\dagger	U	V	W	X	Y	Z	T_{eff} [K]	L_{bol} [L_\odot]	Age ‡ [Myr]
	CP-68 1388	K1	112	2.2	-11.3	-21.0	-7.8	43.5	-101.9	-16.7	5080	1.4	7.9/13.2
13	2MASS J11183572-7935548	M4.5	101	4.2	-8.9	-23.8	-11.5	46.2	-84.5	-30.4	3198	0.084	2.6/4.4
16	2MASS J11404967-7459394	M5.5	101	5.8	-13.1	-17.7	-5.3	46.7	-86.7	-22.3	3058	0.011	14.0/...
17	2MASS J11432669-7804454	M4.7	117	1.7	-10.5	-21.7	-8.8	55.2	-98.2	-31.6	3169	0.041	5.8/...
	RX J1147.7-7842	M3.5	106	2.9	-9.6	-20.6	-12.4	50.5	-88.4	-29.6	3343	0.24	0.9/2.2
18	RX J1149.8-7850	M0	110	1.8	-11.2	-18.9	-10.8	52.5	-91.5	-31.0	3850	0.44	2.1/2.9
	RX J1150.9-7411	M3.7	108	4.6	-10.7	-22.0	-5.6	50.9	-92.7	-22.1	3314	0.092	4.0/5.2
	2MASS J11550485-7919108	M3	115	1.8	-11.2	-20.6	-8.1	55.4	-95.1	-33.1	3415	0.092	6.7/6.6
	T Cha	K0	108	0.9	-11.1	-19.8	-10.5	52.2	-89.2	-31.1	5250	1.2	13.3/20.7
20	RX J1158.5-7754B	M3	119	2.2	-11.3	-18.6	-11.1	57.5	-99.3	-31.5	3415	0.15	2.9/3.9
21	RX J1158.5-7754A	K4	104	4.7	-13.0	-17.6	-6.8	50.3	-86.8	-27.5	4590	0.75	7.2/...
	HD 104036	A7	108H	3.3	-12.4	-18.3	-11.9	52.4	-90.5	-28.5	7850	20.0	6.3/7.2
2	ϵ Cha AB	B9	110H	2.8	-12.0	-18.8	-11.8	53.7	-92.3	-29.9	10500	99.9	2.6/2.8
	RX J1159.7-7601	K4	107	0.6	-11.1	-19.9	-10.1	51.6	-90.3	-24.9	4590	0.50	14.4/14.4
3	HD 104237C	M/L	114H	55.6	-95.4	-30.8
4	HD 104237B	K/M	114H	55.6	-95.4	-30.8
5	HD 104237A	A7.75	114H	1.3	-11.6	-20.1	-10.9	55.6	-95.4	-30.8	7648	38.6	3.6/3.9
6	HD 104237D	M3.5	114H	55.6	-95.4	-30.8	3343	0.11	3.3/4.6
7	HD 104237E	K5.5	114H	55.6	-95.4	-30.8	4278	0.74	3.2/5.2
10	2MASS J12005517-7820296	M5.75	126	4.5	-12.8	-18.3	-6.4	61.2	-104.7	-34.2	3024	0.032	2.8/...
	HD 104467	G3	102	2.1	-12.0	-18.8	-9.3	49.6	-84.4	-28.7	5830	4.0	8.1/12.3
11	2MASS J12014343-7835472	M2.25	100	5.7	-8.0	-24.7	-12.3	48.6	-82.9	-27.5	3524	0.0029	...
8	USNO-B 120144.7-781926	M5	100	1.5	-10.8	-21.4	-8.7	48.6	-83.1	-27.1	3125	0.027	7.9/8.9
9	CXOU J120152.8-781840	M4.75	121	3.0	-9.4	-21.4	-12.3	58.9	-100.5	-32.7	3161	0.042	5.5/7.1
	RX J1202.1-7853	M0	110	2.9	-9.6	-23.1	-9.7	53.6	-91.0	-30.8	3850	0.43	2.2/3.0
	RX J1204.6-7731	M3	112	4.0	-12.9	-17.6	-7.8	54.7	-93.4	-28.8	3415	0.22	1.4/2.5
	RX J1207.7-7953	M3.5	111	1.2	-10.5	-20.6	-11.0	54.5	-91.0	-32.8	3343	0.11	3.3/4.5
	HD 105923	G8	112	0.7	-10.7	-21.0	-9.6	54.9	-96.2	-16.7	5520	3.3	5.6/10.5
	RX J1216.8-7753	M4	118	0.6	-10.8	-20.1	-10.5	58.8	-97.6	-30.8	3270	0.17	1.2/2.9
	RX J1219.7-7403	M0	112	0.6	-11.0	-20.7	-9.4	56.1	-94.4	-22.0	3850	0.28	5.5/5.9
	RX J1220.4-7407	M0	110	2.2	-11.9	-19.8	-8.1	55.2	-92.7	-21.7	3850	0.36	3.3/4.0
	2MASS J12210499-7116493	K7	110	2.0	-11.8	-18.7	-10.2	55.2	-93.7	-16.4	4060	0.53	3.1/4.5
	RX J1239.4-7502	K3	100	1.2	-10.7	-21.2	-9.0	52.0	-82.8	-21.1	4730	0.96	6.6/...
	CD-69 1055	K0	99	0.6	-10.7	-21.0	-9.8	54.2	-81.8	-13.1	5250	1.5	9.3/15.6
	MP Mus	K1	101	0.2	-10.7	-20.6	-9.9	58.4	-81.5	-12.2	5080	1.3	8.6/14.1

(*) Suffix 'H' denotes a trigonometric distance from *Hipparcos*. All other distances are kinematic.

(†): Difference between the star and mean ϵ Cha space motion, see §4.4.

(‡): Ages estimated from the Dotter et al. (2008) and Siess et al. (2000) models, respectively.

(GSC 9415-2676, $d_{\text{kin}} = 119$ pc). Perhaps as well as being responsible for the velocity variation (Table 5), the close companion distorted the parallax over the short-baseline *Hipparcos* observations. The triple system is only 5 arcmin from HD 104036, which has a *Hipparcos* distance of 108 ± 4 pc.

HD 104237A (ϵ Cha 5): A core member of ϵ Cha, the Herbig Ae star has a space motion only 1.3 km s^{-1} from the mean and a kinematic distance which agrees with its 114 pc *Hipparcos* parallax. HD 104237A was rejected in the convergent analysis because of its position above the isochrone. This is likely due to a combination of binarity (Böhm et al. 2004), infrared excess and an uncertain spectral type (Lyo et al. 2008).

HD 104237B-E (ϵ Cha 3-7): All four late-type components of the HD 104237 system show X-ray emission and are almost certainly associated with their primary. Fang et al. (2013) recently estimated the mass of HD 104237C to be $13\text{--}15 M_{\text{Jup}}$ from near-infrared photometry, making it the lowest-mass member of ϵ Cha. Components D and E have strong lithium absorption. Both stars were rejected from the convergent solution by their discrepant kine-

matics. Their proper motions (and the photometry of HD 104237D) are likely influenced by the proximity of HD 104237A.

2MASS J12014343-7835472 (ϵ Cha 11): We find an excellent proper motion match at 100 pc with a predicted radial velocity 6 km s^{-1} lower than measured. This may be due to unresolved binarity or strong accretion activity (see §6.3). Three WiFeS velocities showed no trend over ~ 1 yr. Luhman (2004b) attributed its under-luminosity to obscuration by an edge-on circumstellar disc. This was confirmed by Fang et al. (2013). We confirm membership in ϵ Cha based on a congruent proper motion, Li I equivalent width and location in the core of the association.

5.1.2 Provisional members

CXOU J115908.2-781232 (ϵ Cha 1): The smaller proper motion yields a kinematic distance of 165 pc ($K = 5.2 \text{ km s}^{-1}$). The star is unlikely to have been ejected from the core as its predicted radial velocity is only $\sim 1 \text{ km s}^{-1}$ from observed. ϵ Cha 1 is not found in UCAC4 but its PPMXL proper motion ($\mu_{\alpha \cos \delta}, \mu_{\delta} = -36 \pm 14, -6 \pm 14 \text{ mas yr}^{-1}$) is consistent with membership at 120 pc

Table 8. Provisional members of the ϵ Cha association requiring confirmation

ID	Name	Spec. Type	Dist.* [pc]	K^\dagger	U	V	W	X	Y	Z	T_{eff} [K]	L_{bol} [L_\odot]	Age ‡ [Myr]
1	TYC 9414-191-1	K5	105	47.4	-88.9	-29.7	4350	1.2	1.6/3.1
	CXOU J115908.2-781232	M4.75	165	5.2	-10.2	-22.4	-5.1	79.9	-137.4	-44.4	3161	0.055	3.8/5.8
	RX J1202.8-7718	M3.5	128	3.0	-9.7	-23.1	-9.7	62.3	-107.0	-32.5	3343	0.14	2.2/...
	HD 105234	A9	103H	50.5	-85.1	-28.5	7390	9.4	10.0/...
	HIP 59243	A6	94H	46.2	-77.5	-26.0	8350	15.8	7.9/9.0
	CM Cha	K7	133	5.2	-9.3	-23.9	-6.4	71.4	-107.6	-31.7	4060	0.49	3.7/5.1

(*): Suffix ‘H’ denotes a trigonometric distance from *Hipparcos*. All other distances are kinematic.

(†): Difference between the star and mean ϵ Cha space motion, see §4.4.

(‡): Ages estimated from the Dotter et al. (2008) and Siess et al. (2000) models, respectively.

($K = 1.5 \text{ km s}^{-1}$), notwithstanding the large errors. Membership in Cha I or II is unlikely. Given its location near the centre of ϵ Cha we assign it provisional membership pending better kinematics.

RX J1202.8-7718: In the absence of accelerated lithium depletion (e.g. Baraffe & Chabrier 2010) the star’s 300 mÅ Li I λ 6708 equivalent width suggests an age closer to the TW Hya and β Pic associations (8–12 Myr). The only nearby population with a similar age is the Lower Centaurus Crux (LCC) subgroup of Sco-Cen, whose southern extent may be as young as ~ 10 Myr (see §8). RX J1202.8-7718 is an equally good match to the LCC space motion (Chen et al. 2011) at 110 pc. Given its location close to the core of ϵ Cha we retain it as a provisional member, though it may be an older, dispersed member of Sco-Cen.

CM Cha: Previously assigned to Cha II, the star was tentatively reclassified as a member of ϵ Cha by Lopez Martí et al. (2013) by its UCAC3 proper motion. With SPM4 we find a somewhat poor ($K = 5.2 \text{ km s}^{-1}$) kinematic match to ϵ Cha at 133 pc. A marginally better match to Cha II (Lopez Martí et al. 2013) is found at ~ 120 pc, though this is considerably closer than recent distance estimates to the cloud (180–210 pc; Knude 2010). Given its location near Cha II and discordant proper motions (see §4.1.2) we assign provisional membership in ϵ Cha and await improved kinematics or a parallax.

5.1.3 Non-members

HD 82879: The F6 star is only 24 arcsec from and comoving with HD 82859 (F4, Fig. 12). It is associated with the *ROSAT* X-ray source RX J0928.5-7815 and was proposed as an ϵ Cha member by Torres et al. (2008). Lopez Martí et al. (2013) also listed it as a member but neither study noted its binarity. HD 82879 is young and a good kinematic match to ϵ Cha. However, given its large total mass ($\sim 2.8 M_\odot$) and isolation it is unlikely the system could have been dispersed from ϵ or η Cha within their lifetimes. Furthermore, at its 120 pc kinematic distance HD 82879 has an isochronal age of 18–25 Myr (see §6.1). The non-detection of either star by *Hipparcos* means they are likely to be significantly further away. da Silva et al. (2009) suggested HD 82879 as a member of the AB Dor association, however we find a poor kinematic match at any distance. Spectroscopy of HD 82859 would be useful.

HIP 55746: This star has the largest offset from the mean ϵ Cha space motion ($K = 6.7 \text{ km s}^{-1}$) and is the closest proposed member ($89 \pm 5 \text{ pc}$, *Hipparcos*). However, it is only 3 km s^{-1} from the space motion of AB Dor (Torres et al. 2008) with a distance similar to other members. We follow Torres et al. (2008) and assign the star to AB Dor.

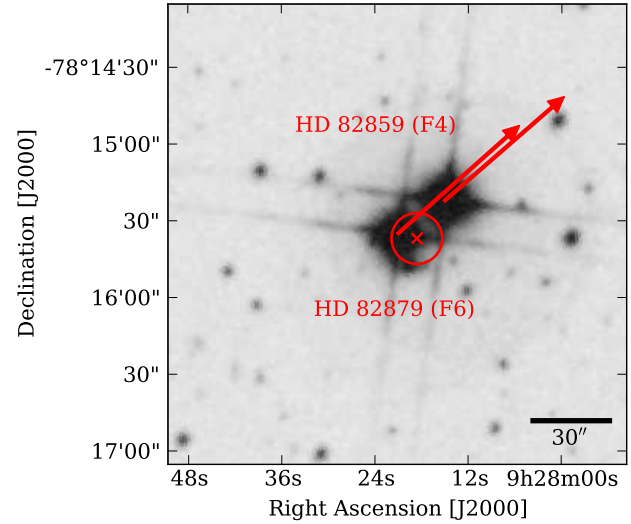


Figure 12. POSS2-Red 3×3 arcmin image centred on HD 82879. Arrows show the Tycho-2 proper motions over 2000 yr. The cross and circle give the position of the *ROSAT* source (RX J0928.5-7815) and its uncertainty.

RX J1137.4-7648: Despite the excellent kinematic match ($K=1.7 \text{ km s}^{-1}$), the 4 mag under-luminosity, outlying distance (67 pc) and lack of Li I λ 6708 absorption conclusively rule RX J1137.4-7648 out as a member of ϵ Cha. The 3-arcsec visual binary is likely an nearby, older field system.

2MASS J11334926-7618399 (ϵ Cha 15): Located between Cha I and the core of ϵ Cha, the star was proposed by Luhman et al. (2008) as having a proper motion (not reported in that work) more similar to ϵ Cha than the cloud sources. Although it lies on the isochrone only 2.6 km s^{-1} from the mean ϵ Cha space motion, its 197 pc distance is much greater than other members. The star is not in the USNO-B1 or UCAC catalogues and its SuperCosmos proper motion is erroneous. Its PPMXL and SPM4 kinematics and the modest reddening we measured are consistent with an outlying Cha I member at a distance of ~ 160 pc.

RX J1243.1-7458: The close binary (Köhler 2001) lies a few degrees north of Cha II and its space motion gives a reasonable agreement ($K = 3.7 \text{ km s}^{-1}$) with the cloud sources at ~ 260 pc. This is considerably larger than recent distance estimates to the cloud (180–210 pc; Knude 2010). If we use the Terranegra et al. (1999) proper motion a better match is found at 200 pc. The predicted radial velocity agrees with the mean WiFeS value, implying

Table 9. Candidates from the literature rejected as ϵ Cha members

ID	Name	Reason [†]	Membership
	HD 82879/82859	Binary	? Young
	RX J1137.4–7648	ΔM_I , dist, Li	Old field
	HIP 55746	...	AB Dor
15	2MASS J11334926–7618399	dist	Cha I
	VW Cha	ΔM_I , dist	Cha I
	RX J1243.1–7458	dist	Cha II
14	RX J1123.2–7924	ΔM_I , Li	Octans?
12	2MASS J12074597–7816064	ΔM_I	? Young
19	RX J1150.4–7704	ΔM_I	? Young
	TYC 9238-612-1	ΔM_I	?
	TYC 9420-676-1	ΔM_I	?

([†]) ΔM_I : Photometry >1 mag from isochrone, dist = bad kinematic distance, Li = incongruous Li I $\lambda 6708$ equivalent width

we observed the star close to its systemic velocity. We classify RX J1243.1–7458 as an outlying member of Cha II, but caution that its proper motions may be affected by the close companion.

VW Cha: The star is unlikely to be a member of ϵ Cha based on its large implied distance (217 pc) and position well above the isochrone. It was classified as a Cha I member by Luhman (2007) and again by Lopez Martí et al. (2013). Its proper motion, large extinction and location inside the southern cloud core support this assignment. We find the best match to the Cha I space motion (Lopez Martí et al. 2013) at ~ 160 pc, the distance to the cloud.

RX J1150.4–7704 (ϵ Cha 19): Torres et al. (2008) rejected membership in ϵ Cha on the basis of a -3.3 ± 1.0 km s⁻¹ velocity from Guenther et al. (2007), but this was almost certainly not systemic, nor is the mean WiFeS value. At its 106 pc kinematic distance RX J1150.4–7704 lies 1.4 mag below the isochrone, more if its unresolved companion contributes significantly to the I -band flux. Despite strong lithium absorption and a congruent proper motion we rule out membership in ϵ Cha. A systemic velocity would be useful. Wahhaj et al. (2010) classified the star as T Tauri based on a broad H α line, but this is likely the result of binarity.

2MASS J12074597–7816064 (ϵ Cha 12): A proper motion outlier, ϵ Cha 12 also shows evidence of spectroscopic binarity. We find a good match to the ϵ Cha space motion at 85 pc, but the star is under-luminous at this distance. It is located in the core of the association and its strong lithium absorption implies an age comparable to other members. The companion may have influenced the star's proper motions but even at 110 pc ϵ Cha 12 remains significantly under-luminous. We refrain from assigning it to ϵ Cha pending better kinematics and confirmation of binarity.

RX J1123.2–7924 (ϵ Cha 14): Lopez Martí et al. (2013) reaffirmed membership in ϵ Cha based on a marginally-consistent proper motion. The star's low Li I equivalent width (150 mÅ) and position below the isochrone mean it is unlikely to be a member of ϵ Cha, nor the young groups in the vicinity. Although the proper motion may have been influenced by the unresolved companion, we did find an excellent match to the ~ 20 Myr-old Octans association (Torres et al. 2008) at 110 pc. The lithium depletion, CMD placement and Galactic position of RX J1123.2–7924 are consistent with this assignment. A systemic velocity is necessary to confirm its true kinematics and membership.

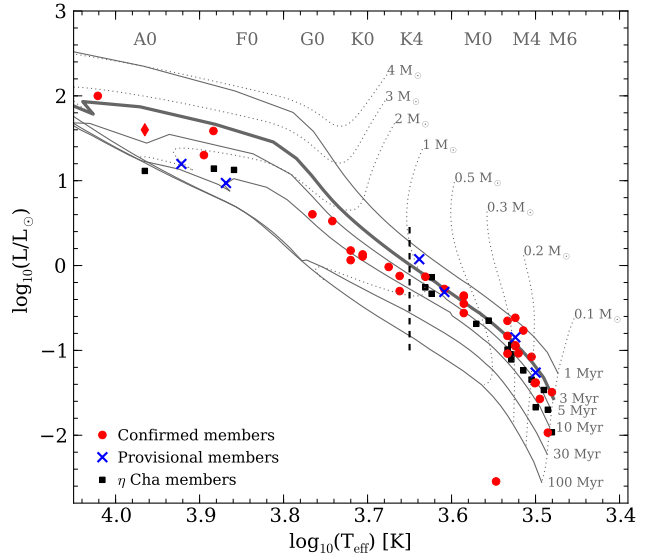


Figure 13. HR diagram of confirmed ϵ Cha members (red circles), provisional members (crosses) and η Cha members (squares). The filled diamond is ϵ Cha B. Its position was estimated from the photometry and spectral type in Feigelson et al. (2003). Pre-main sequence mass tracks and isochrones from Dotter et al. (2008) are plotted for comparison. The dashed line at $\log_{10} T_{\text{eff}} = 3.65$ is the limit of the low-mass sample (see text).

5.1.4 Candidates without radial velocities

The five candidates without radial velocities are plotted separately in Fig. 10. To calculate kinematic distances for these stars we compared their proper motions to the ϵ Cha solution or used parallaxes if available. TYC 9414-191-1, HD 105234 and HIP 59243 may be members based on their kinematic match and CMD placement. Radial velocities and a Li I $\lambda 6708$ measurement for TYC 9414-191-1 are necessary to confirm membership. The two remaining Tycho sources have positions below the empirical isochrone.

5.2 Final membership of ϵ Cha

Our updated membership for ϵ Cha contains 35 stars; 29 from the kinematic solution plus 2MASS J12014343–7835472 (ϵ Cha 11) and HD 104237A–E. The heliocentric positions and velocities of these stars are plotted in Fig. 8 and listed in Table 7. Six candidates (CXOU J115908.2–781232, RX J1202.8–7718, CM Cha, TYC 9414-191-1, HD 105234 and HIP 59243) are provisional members requiring further observation. They are also plotted in Fig. 8 and listed in Table 8. The 11 stars unlikely to be members are summarised in Table 9 with suggested membership assignments.

6 DISCUSSION

6.1 Age of ϵ Cha

Fig. 13 shows the HR diagram for confirmed and provisional members of ϵ Cha. The effective temperature of each star was obtained from its spectral type using the temperature scales of Kenyon & Hartmann (1995) for spectral types earlier than M1 and Luhman et al. (2003) for M1–M6. For TYC 9414-191-1 we adopted a spectral type of K5 ($A_V = 0.9$) which is consistent with its $B - V$ colour and position in Fig. 4. Luminosities were

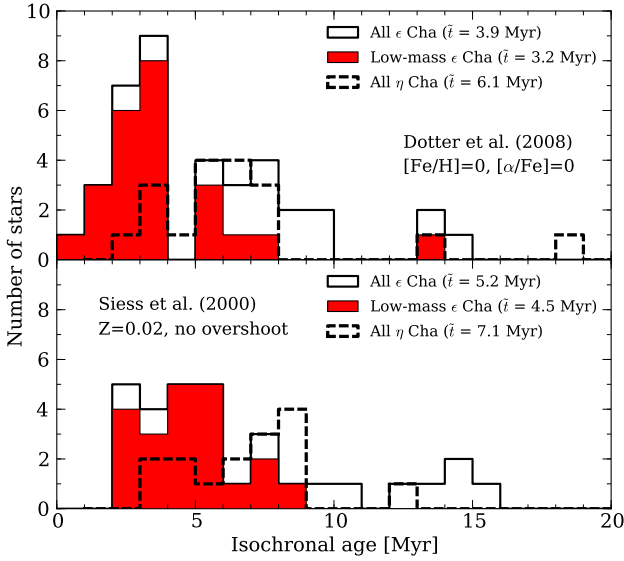


Figure 14. Ages derived from the Dotter et al. (2008) (top panel) and Siess et al. (2000) (bottom panel) isochrones. Stars with $\log_{10} T_{\text{eff}} < 3.65$ are shown in red, the solid line is the envelope of all members. Dashed lines are η Cha members. Median ages are given in the legend.

calculated using de-reddened J -band magnitudes and the bolometric corrections (BC) of Kenyon & Hartmann (1995). We adopted $M_{\text{bol},\odot} = 4.64$, appropriate for the Kenyon & Hartmann BC scale. Pre-main sequence isochrones and evolutionary tracks from Dotter et al. (2008) are plotted for comparison.⁵ The four early type members fall around the 3–5 Myr isochrones, as do the majority of late-type stars. The solar-type members of ϵ Cha appear systematically older in this diagram, with ages of 5–10 Myr.

Individual ages were obtained by interpolating the isochrones at the position of each star. The resulting age distribution is plotted in the top panel of Fig. 14. The median age of all members is 4^{+4}_{-2} Myr⁶. If we restrict our sample to stars with $\log T_{\text{eff}} < 3.65$ (approximately K4 spectral type and later) the spread is much reduced and the median age is 3^{+2}_{-1} Myr. These agree with previous isochronal age estimates using fewer stars (Fang et al. 2013) and different model grids (Feigelson et al. 2003; Luhman 2004b). As a check we also calculated ages using the isochrones of Siess et al. (2000) (Fig. 14, bottom panel). The distribution is less-peaked but both sets of models indicate ϵ Cha has a median age of 3–5 Myr. This makes it the youngest association in the solar neighbourhood ($\lesssim 100$ pc) and its members ideal targets for high-sensitivity studies of young stars, their discs and nascent planetary systems.

As they are commonly cited as being coeval (e.g. Torres et al. 2008) it is worthwhile to compare the ages of η and ϵ Cha. We conducted a similar analysis using the 18 core members of η Cha, adopting spectral types from Luhman & Steeghs (2004), a distance of 94 pc and correcting the photometry of the equal-mass binaries RECX 1, 9 and 12. Both the HR diagram and resulting age distributions suggest a small (1–3 Myr) age difference, with η Cha having a median age of 6^{+2}_{-3} Myr (Dotter et al. 2008) and 7^{+1}_{-3} Myr

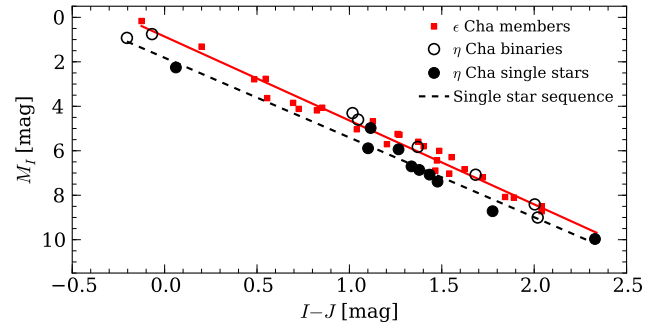


Figure 15. Colour-magnitude diagram with confirmed members of ϵ Cha (red squares) and the eight binary (Lyo et al. 2004b, open circles) and 10 single members of η Cha (filled circles). As predominantly equal-mass systems the binaries follow a sequence ~ 0.75 mag above the single stars.

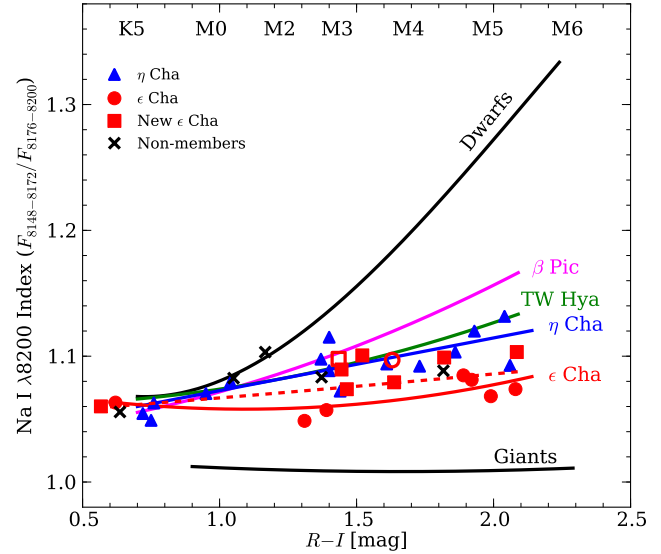


Figure 16. Na I $\lambda 8200$ gravity indices of young associations. Solid lines are mean trends from Lawson et al. (2009), with η and ϵ Cha members from Lyo et al. (2004a, 2008) (filled circles, triangles) and new ϵ Cha members observed with WiFeS (filled squares). Open symbols are the non-member 2MASS J12074597-7816064 (ϵ Cha 12) and provisional member RX J1202.8-7718. The dashed line is the new fit to all ϵ Cha members.

(Siess et al. 2000). These agree with previous estimates. The small age difference is also apparent in the CMD of both groups (Fig 15), where the sequence of single (or high mass-ratio binary) η Cha members (Lyo et al. 2004b) lies approximately 0.5–1 mag below the ϵ Cha sequence. Comparison against theoretical models again suggests an age difference of 1–3 Myr.

The strength of the Na I $\lambda 8183/8195$ doublet is highly dependent on surface gravity in mid-to-late M-type stars. It can therefore be used as an age proxy for pre-main sequence stars contracting towards their main sequence radii. Lawson et al. (2009) used Na I strengths to rank the ages of several young associations. Their mean trends (Fig. 16) agree with the isochronal and lithium depletion age rankings of the groups. Furthermore, they resolved η and ϵ Cha in gravity, with the former appearing several Myr older. We computed the same Na I index, $\int_{8148}^{8172} F_{\lambda} d\lambda / \int_{8176}^{8200} F_{\lambda} d\lambda$, after smoothing the WiFeS spectra to the $R \approx 800$ resolution of the Lawson et al. data and resampling to the same wavelength scale. Despite the large

⁵ Although isochrones are only provided for $t > 250$ Myr, the tracks contain the full pre-main sequence evolution. We created isochrones from 0.9–100 Myr ($\Delta \log t = 0.1$ Myr) by interpolating the tracks over 0.1–5 M_{\odot} .

⁶ As a measure of dispersion we adopted the 68 per cent confidence interval around the median in the cumulative distribution.

scatter, the revised ϵ Cha trend is still clearly younger than η Cha, confirming the previous HRD and CMD analyses.

6.2 Circumstellar discs in ϵ Cha

To check for circumstellar disc emission we cross-matched the members against 3.4, 4.6, 11.6, and 22.1 μm photometry from the *Wide-field Infrared Survey Explorer* (WISE) All Sky Data Release (Wright et al. 2010). The components of HD 104237 were not resolved individually at the 6–12 arcsec resolution of *WISE*. Spectral energy distributions (SEDs) of the 13 members with infrared excesses are plotted in Fig. 17. Also plotted is the SED of HD 104237E (ϵ Cha 7), which has a clear disc excess from 3–24 μm photometry reported by Grady et al. (2004) and Luhman et al. (2010). Grady et al. also reported strong excess K_s and L' emission from HD 104237B (ϵ Cha 4). The variety of SED morphologies in Fig. 17 is typical of rapidly-evolving intermediate-age discs (Williams & Cieza 2011) and the manifold physical processes (photo-evaporation, accretion, grain growth, dynamical interactions with companions) shaping them. A similar range of discs are observed in η Cha (Sicilia-Aguilar et al. 2009).

Fang et al. (2013) recently presented *Spitzer Space Telescope* IRS spectroscopy of ten members (ϵ Cha 1,2,5–12). Their 7–35 μm spectrum of CXOU J115908.2–781232 (ϵ Cha 1) and preliminary *WISE* photometry showed no excess emission above photospheric levels, whereas with the final *WISE* release there is a clear excess at 22 μm . USNO-B 120144.7–781926 (ϵ Cha 8) and 2MASS J12005517–7820296 (ϵ Cha 10) show signs of reduced disc heights due to dust settling (homologous depletion), and the disc around HD 104237E (ϵ Cha 7) may be undergoing partial dissipation in its inner regions, leaving the outer disc intact (inside-out evolution). Fang et al. (2013) attributed the under-luminosity of 2MASS J12014343–7835472 (ϵ Cha 11) to a flared disk seen at moderately-high inclination ($\sim 85^\circ$), in which the central star is seen in only scattered light but the majority of the infrared disk emission is allowed through.

2MASS J11183572–7935548 (ϵ Cha 13) and 2MASS J11432669–7804454 (ϵ Cha 17) were classified by Luhman et al. (2008) as Class II sources and confirmed with *Spitzer* IRS by Manoj et al. (2011). ϵ Cha 17 is a transitional disc candidate with a strong 10 μm silicate feature. RX J1149.8–7850 (ϵ Cha 18) was classified by Luhman et al. (2008) as having a Type I/II flat SED.

The SED of T Cha B (2MASS J11550485–79191081) was well-fitted with a spectral type of M3 and extinction of $A_V \approx 1.6$, the same as that adopted for T Cha (and consistent with Fig. 4). T Cha is subject to varying degrees of obscuration by circumstellar material (Schisano et al. 2009) whereas the lack of near-infrared excess in T Cha B usually implies a disc with an inner opacity hole.

The provisional member HD 105234 is surrounded by a warm, gas-poor debris disc (Currie et al. 2011). Unlike most debris discs it also has numerous solid-state features, including a pronounced 10 μm silicate feature. This is evidence for the presence of small, μm -sized grains. The optically-thick accretion disc around provisional member CM Cha is consistent with membership in the younger Cha II cloud as well as ϵ Cha.

MP Mus was classified by Mamajek et al. (2002) as a 7–17 Myr-old member of LCC but its optically-thick accretion disc is more consistent with the younger age of ϵ Cha. Such discs are rare around stars older than 5–10 Myr and MP Mus was the only accretor with a K -band excess detected by Mamajek et al. from 110 solar-type members of Sco-Cen. Moreover, their ~ 86 pc kinematic

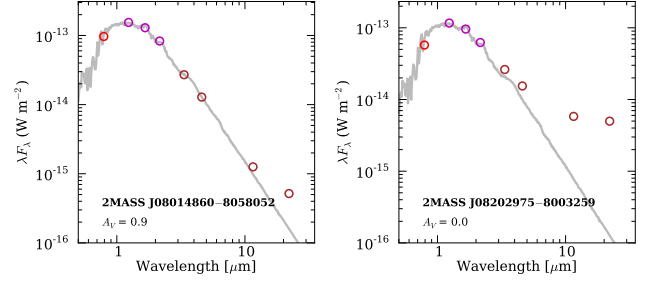


Figure 18. Same as Fig. 17, for the η Cha halo members 2MASS J08202975–8003259 and 2MASS J08014860–8058052. After reconsidering its photometry and optical spectrum 2M J0801–80 has a spectral type of M4 and $A_V \approx 0.9$ (c.f. Murphy et al. 2010).

distance made MP Mus the third-closest member of LCC whereas our 101 pc distance is entirely consistent with ϵ Cha.

Two candidates reclassified as Cha I members have infrared excesses. The SEDs of 2MASS J11334926–7618399 (ϵ Cha 15) and VW Cha are plotted in Fig. 17. We also constructed SEDs for the new halo members of η Cha (Murphy et al. 2010). The two stars with detectable excesses are shown in Fig. 18. While 2MASS J08202975–8003259 was easily visible in the preliminary *WISE* release (Simon et al. 2012), the small 22 μm excess in 2MASS J08014860–8058052 is a new detection.

6.2.1 Circumstellar disc frequency

Fang et al. (2013) reported a disc frequency of 55^{+13}_{-15} per cent (6/11) for the 12 classical members of ϵ Cha. If we consider all 41 confirmed and provisional members there are 12 stars with disc excesses at wavelengths shorter than ~ 8 μm (corresponding to the *Spitzer* IRAC bands), giving a disc frequency of 29^{+8}_{-6} per cent⁷. This is likely an upper limit as the complete membership of ϵ Cha is still unknown. However, if like Fang et al. (2013) we assume the well-studied region within 0.5 deg of HD 104237 to be essentially complete (Fig. 1) then the disc fraction increases to 43^{+13}_{-11} per cent (6/14). While lower than that reported by Fang et al., it is still larger than the 10–30 per cent frequency predicted for a 3–5 Myr-old population by the exponential relationship of Fedele et al. (2010). After also considering the large fraction of accreting stars in ϵ Cha (§6.3) Fang et al. (2013) concluded that discs in sparse associations evolve more slowly than in denser environments. Given the small number of stars and the incomplete memberships of ϵ Cha and other young associations this conclusion requires further testing.

6.3 Classical T Tauri stars in ϵ Cha

The strength of $H\alpha$ emission is commonly used to identify Classical T Tauri (CTT) stars actively accreting from circumstellar discs. Confirmed or provisional members of ϵ Cha with $H\alpha$ data are plotted in Fig 19. By the equivalent width criteria proposed by Fang et al. (2009) 10 stars have $H\alpha$ emission in excess of chromospheric activity and are likely accreting. Unsurprisingly, all of these stars also show strong disc excesses. Though unresolved by *WISE*, HD 104237E (ϵ Cha 7) is also accreting based on its disc excess and broad ($v_{10} \approx 500 \text{ km s}^{-1}$) $H\alpha$ line reported by Feigelson et al.

⁷ Uncertainties for small samples are calculated for 68 per cent confidence intervals following the prescription of Cameron (2011).

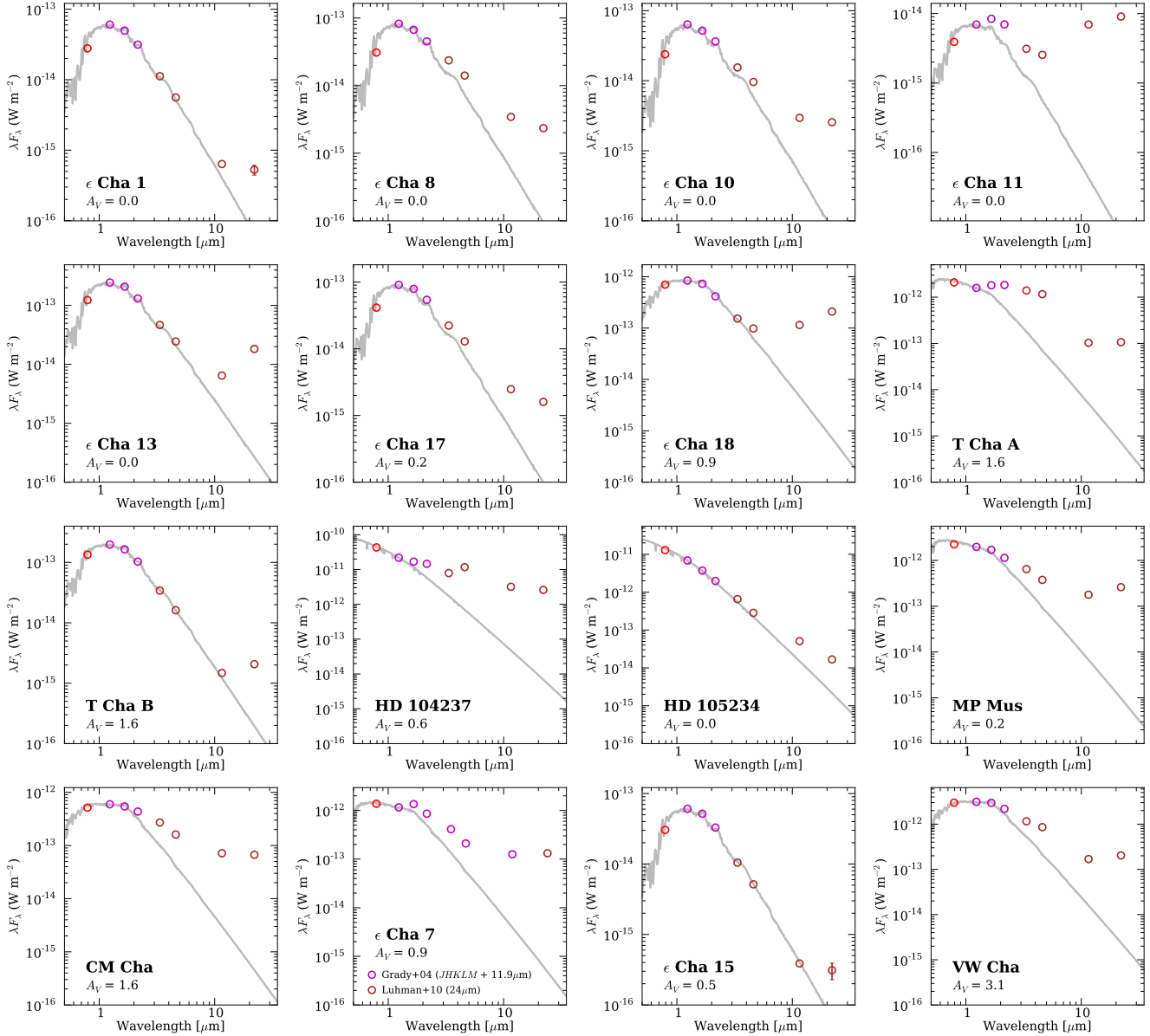


Figure 17. De-reddened DENIS (i , red circle), 2MASS (JHK_s , magenta points) and WISE ($W1$ – $W4$, brown points) 0.7–22 μm spectral energy distributions of those ϵ Cha members with an infrared excess. Isophotal wavelengths and zero magnitude fluxes were taken from Fouqué et al. (2000), Cohen et al. (2003) and Jarrett et al. (2011). Flux errors are within the plotted points unless shown. The photospheric flux (grey line) is approximated by a solar metallicity, $\log g = 4.5$ MARCS model (Gustafsson et al. 2008) with similar effective temperature scaled to the J -band magnitude of each star. Photometry for ϵ Cha 7 (HD 104237E) comes from Grady et al. (2004) and Luhman et al. (2010). ϵ Cha 15 and VW Cha are kinematic members of Cha I.

(2003). The equivalent width of 2MASS J11404967–7459394 (ϵ Cha 16) flared to -35 \AA on 2011 June 19 from its quiescent level around -11 \AA . The star has no infrared excess and its H α emission is likely chromospheric in origin.

Our multi-epoch WiFeS observations revealed three CTT members with broad, variable H α emission. Velocity profiles of those stars are plotted in Fig. 20. They show asymmetric, multi-component emission and velocity widths at 10 per cent of peak flux (v_{10}) in excess of the $v_{10} = 200$ – 270 km s^{-1} accretion threshold (Jayawardhana et al. 2003). Note the large *daily* variation in the triple-peaked profiles of ϵ Cha 8. All three stars also exhibited He I $\lambda 5876/6678$ emission and ϵ Cha 11 displayed strong forbidden [O I] $\lambda 6300/6363$ and [N II] $\lambda 6584$ emission. Using the v_{10} veloc-

ity widths and the relation of Natta et al. (2004), the accretion rates in these stars are $\sim 10^{-10}$ – $10^{-8.5} M_{\odot} \text{ yr}^{-1}$, 1–2 orders of magnitude larger than those in η Cha (Lawson et al. 2004; Murphy et al. 2011) and the TW Hya association (Muzerolle et al. 2000).

The spectrum of 2MASS J11183572–7935548 (ϵ Cha 13) is unique amongst ϵ Cha members, with strong H α , Na I D, He I and forbidden [O I], [O II] $\lambda 7320/7331$, [N II] $\lambda 6548/6583$, [S II] $\lambda 6716/6731$, [Ca II] $\lambda 7291/7324$ and [Fe II] $\lambda 7155$ emission lines all present (Fig. 21). While the emission was persistent over our 2010–11 observations it is obviously variable as only the H α line was present in the discovery spectrum of Luhman (2007). Forbidden emission usually arises in low-density, accretion-driven outflows (Appenzeller & Mundt 1989). The presence of high-

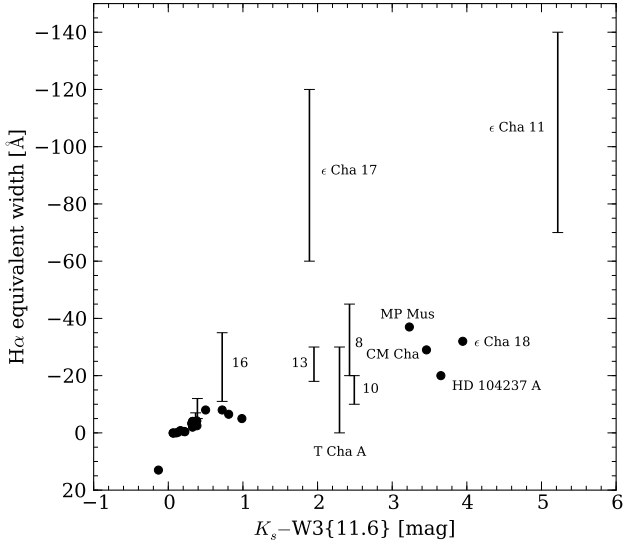


Figure 19. Equivalent width (negative values denote emission) of the $H\alpha$ line versus the 2MASS/WISE $K_s - W3$ colour. With the exception of T Cha, all of the multi-epoch measurements (solid bars) are from our WiFeS/R7000 observations. We classify as CTT members those stars with $K_s - W3 > 1.5$, as well as HD 104237E (ϵ Cha 7).

excitation forbidden [O II] lines requires higher densities than those typically found in protostellar winds and may be evidence for a jet. ϵ Cha 13 has a transitional disc with a large implied inner hole (Manoj et al. 2011). This is consistent with the narrower $H\alpha$ line ($v_{10} \approx 170 \text{ km s}^{-1}$) and smaller accretion rate ($10^{-11} M_{\odot} \text{ yr}^{-1}$). The outflow or jet may be responsible for clearing the inner region of the disc, leaving less material to accrete onto the star.

6.3.1 Accretor frequency

Of the 34 confirmed or provisional members with $H\alpha$ measurements 11 are actively accreting (Fig. 19 plus HD 104237E). This is 32^{+9}_{-7} per cent. Fang et al. (2013) considered the classical membership of the association (ϵ Cha 1–12) and found a value of 63^{+13}_{-18} per cent (5/8). If we again assume the region within 0.5 deg of HD 104237 is complete, then the fraction of accreting members is 45^{+15}_{-13} per cent (5/11). Like the disc fraction, both estimates are larger than the 10–30 per cent predicted by Fedele et al. (2010).

6.4 Binaries in ϵ Cha

Six members of ϵ Cha are confirmed spectroscopic or visual binaries (RX J1158.5–7754A, RX J1220.4–7407, RX J1150.9–7411, RX J1204.6–7731, HD 104237A and ϵ Cha) and four stars are suspected of having a spectroscopic companion (ϵ Cha 10, 13, RX J1202.1–7853 and HD 104467). These give binary fractions of 21^{+10}_{-6} per cent (confirmed) and 36^{+10}_{-8} per cent (including suspected) when compared to the 18 single members with two or more radial velocity measurements. The core of η Cha has a similar binary fraction of 27–44 per cent (Lyo et al. 2004b), but lacks any systems with separations greater than 20 au (Brandeker et al. 2006).

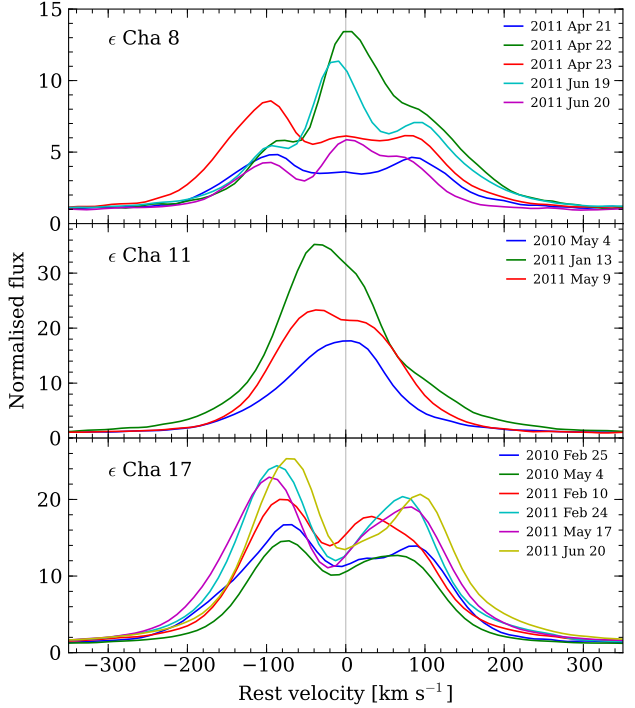


Figure 20. WiFeS/R7000 velocity profiles for ϵ Cha members with complex $H\alpha$ emission lines; USNO-B 120144.7–781926 (ϵ Cha 8), 2MASS J12014343–7835472 (ϵ Cha 11) and 2MASS J11432669–7804454 (ϵ Cha 17). All of the profiles are shifted to zero radial velocity.

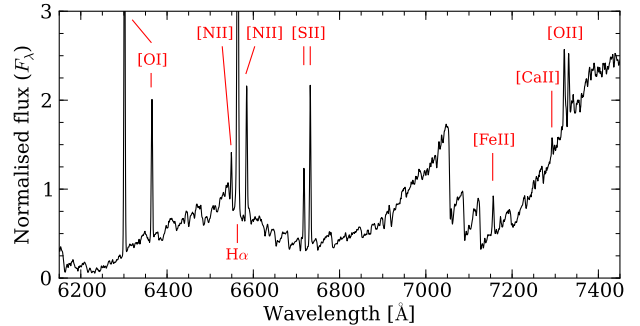


Figure 21. WiFeS/R3000 spectrum of 2MASS J11183572–7935548 (ϵ Cha 13). The star exhibits strong $H\alpha$ and the forbidden line emission typical of a much younger Classical T Tauri (CTT) star.

6.4.1 Wide binaries

There are also several wide systems in ϵ Cha with projected separations of 10^3 – 10^4 au. We have already discussed HD 104237A–E (160–1700 au), RX J1158.5–7754AB (1700 au, hierarchical triple), T Cha AB (0.2 pc; Kastner et al. 2012) and the non-member HD 82879 (F4+F6, 2900 au). In addition to these systems the M0 members RX J1219.7–7403 and RX J1220.4–7407 are separated by only 4.5 arcmin in the north of the association, or 0.14 pc at 110 pc. The latter also has a 0.3 arcsec companion (Köhler 2001). Given their congruent radial velocities, proper motions and isolation they are highly likely to be physically associated.

Although only 6.4 arcmin apart, the *Hipparcos* parallaxes of HD 105234 (A9) and HIP 59243 (A6) differ by 1.6σ (9 ± 2 pc), indicating they are unlikely to be associated. RX J1149.8–7850

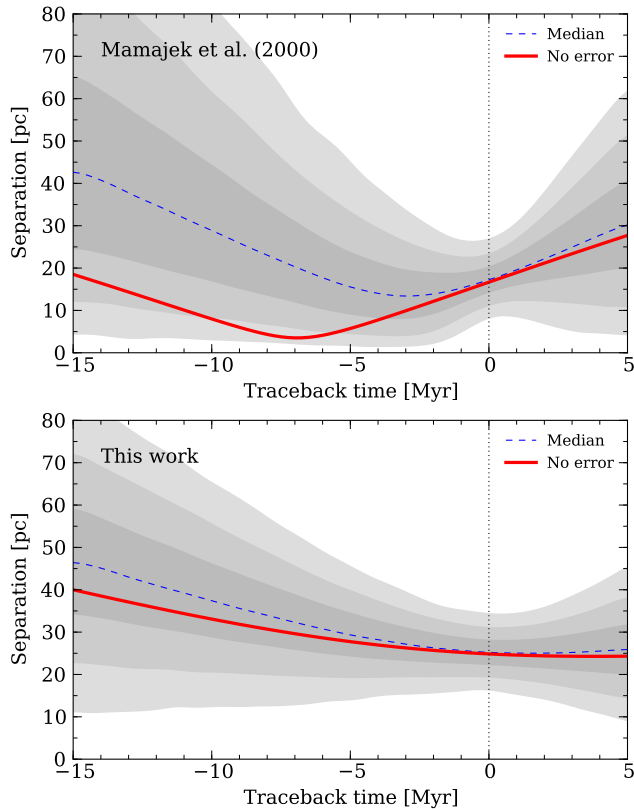


Figure 23. Separation between η Cha and the core of ϵ Cha as a function of time. Top: Initial positions and velocities from Mamajek et al. (2000). Bottom: updated values from Table 6. The solid line assumes no errors on the position or velocity of either association while the shaded regions are the 16–84, 2–98 and 0.1–99.9 per cent contours of the cumulative distribution ($\pm 1-3\sigma$) from 5000 realisations. In both panels the initial centre of ϵ Cha is assumed normally distributed in XYZ with $\sigma = 3$ pc.

(ϵ Cha 18, M0) and RX J1147.7–7842 (M3.5) may form a very wide 10.4 arcmin (0.3 pc) pair at ~ 108 pc although their radial velocities differ by 2.7 ± 1.6 km s $^{-1}$. Similarly, the velocities of HD 104467 and RX J1202.1–7853 (6.4 arcmin) differ by 4.8 ± 1.4 km s $^{-1}$ but both stars are suspected binaries. We note that these three systems are close to the centre of the association where the probability of chance alignment is greater.

7 RELATIONSHIP TO η CHAMAELEONTIS

The core of ϵ Cha lies ~ 10 deg (25 pc) from the young open cluster η Cha (Mamajek et al. 1999). The groups share similar ages, distances and kinematics, which led Torres et al. (2008) to subsume four members of η Cha with radial velocities into their ϵ Cha solution. We did not consider these stars ϵ Cha members in this study. From the age analysis of §6.1 it is now clear that the two groups are distinct, with subtly different space motions, ages and distances. Fig. 22 shows the distribution of η and ϵ Cha members on the sky. Several young low-mass stars have recently been discovered around η Cha (Murphy et al. 2010). They likely trace a comoving halo of members dispersed from the cluster at earlier epochs (but see discussion in Becker et al. 2013).

Using the best-available space motions and positions from Mamajek et al. (2000), Jilinski et al. (2005) showed that the centres of η and ϵ Cha reached a minimum separation of ~ 3 pc some

6–7 Myr ago. They concluded that the groups were born together or very close to one another in the outskirts of Sco-Cen. However, that study did not account for the large errors in the groups’ space motions. Following the prescription of Makarov et al. (2004), our epicyclic traceback analysis (Fig. 23, top panel) replicates the Jilinski et al. result (red line), but shows that such a small separation is unlikely at any epoch given the quoted velocity uncertainties. Around 6–7 Myr ago fewer than 2 per cent of realisations resulted in a separation closer than 3 pc. With improved kinematics and positions for both groups (Table 6), it is clear that η and ϵ Cha were unlikely to have been much closer than their current separation and were ~ 30 pc apart at the time of their birth (Fig. 23, bottom panel). This is further evidence they are distinct entities, albeit with a shared connection to star formation in Sco-Cen (see §8).

Any model for the birth of η and ϵ Cha must also account for their different physical characteristics. For example, to explain η Cha’s apparently primordial deficit of wide (>20 au) binaries (Brandeker et al. 2006) and low-mass objects, Becker et al. (2013) speculated that the cluster was born in a small, highly magnetised cloud which prevented fragmentation on large scales. ϵ Cha was likely born under more quiescent conditions in a less-dense environment, as suggested by its larger spatial extent, the still-bound HD 104237A–E and a number of wider (10^3 – 10^4 au) systems. Moreover, the older wide binaries HD 82879/82859 and RX J0942.7–7726AB (Murphy et al. 2012) as well as several young stars whose origins are as-yet undetermined (e.g. Table 9) are hints that the star-formation history of the region was more complex than the formation of two small groups in isolation a few Myr apart.

8 ϵ CHA AND STAR FORMATION ACROSS THE GREATER SCO-CEN REGION

Immediately north of ϵ Cha is the Lower Centaurus Crux (LCC) subgroup of the Scorpius-Centaurus OB association (Fig. 22). LCC shows signs of spatio-kinematic substructure (Preibisch & Mamajek 2008) whereby the north of the subgroup appears older, richer and more distant (~ 20 Myr, 120 pc) than the south (~ 10 Myr, 110 pc). Recent work has also found a N-S gradient in the W velocity component (E. Mamajek, private communication). These trends may be evidence of a wave of star formation starting in the north 15–20 Myr ago, spreading across the Galactic plane to form the southern part of the subgroup and the β Pic and TW Hya associations ~ 10 Myr ago (Mamajek & Feigelson 2001) and ending with the birth of η and ϵ Cha as recently as 3–5 Myr ago.

Interestingly, 2MASS J12210499–7116493 (Kiss et al. 2011) and four members proposed by Torres et al. (2008) lie north of the majority of ϵ Cha stars within the southern reaches of LCC. Mamajek, Meyer & Liebert (2002) attributed these four stars to LCC in their survey of solar-type Sco-Cen members and they have isochronal ages older than the majority of ϵ Cha members (though this may indicate a problem with the models, see §6.1). Table 10 compares their observed and expected kinematics. With the exception of CP–68 1388, which is a marginally better match to LCC ($\Delta K = 1$ km s $^{-1}$), their proper motions and radial velocities agree with the space motion of ϵ Cha at 100–110 pc. The 80–90 pc distances implied by membership in LCC are at the low end of the 100–120 pc typically attributed to the subgroup. At late-G and early-K spectral types there is little difference in lithium depletion between stars of ages $\lesssim 20$ Myr. However, the K7 2MASS J12210499–7116493 has an Li I equivalent width much greater

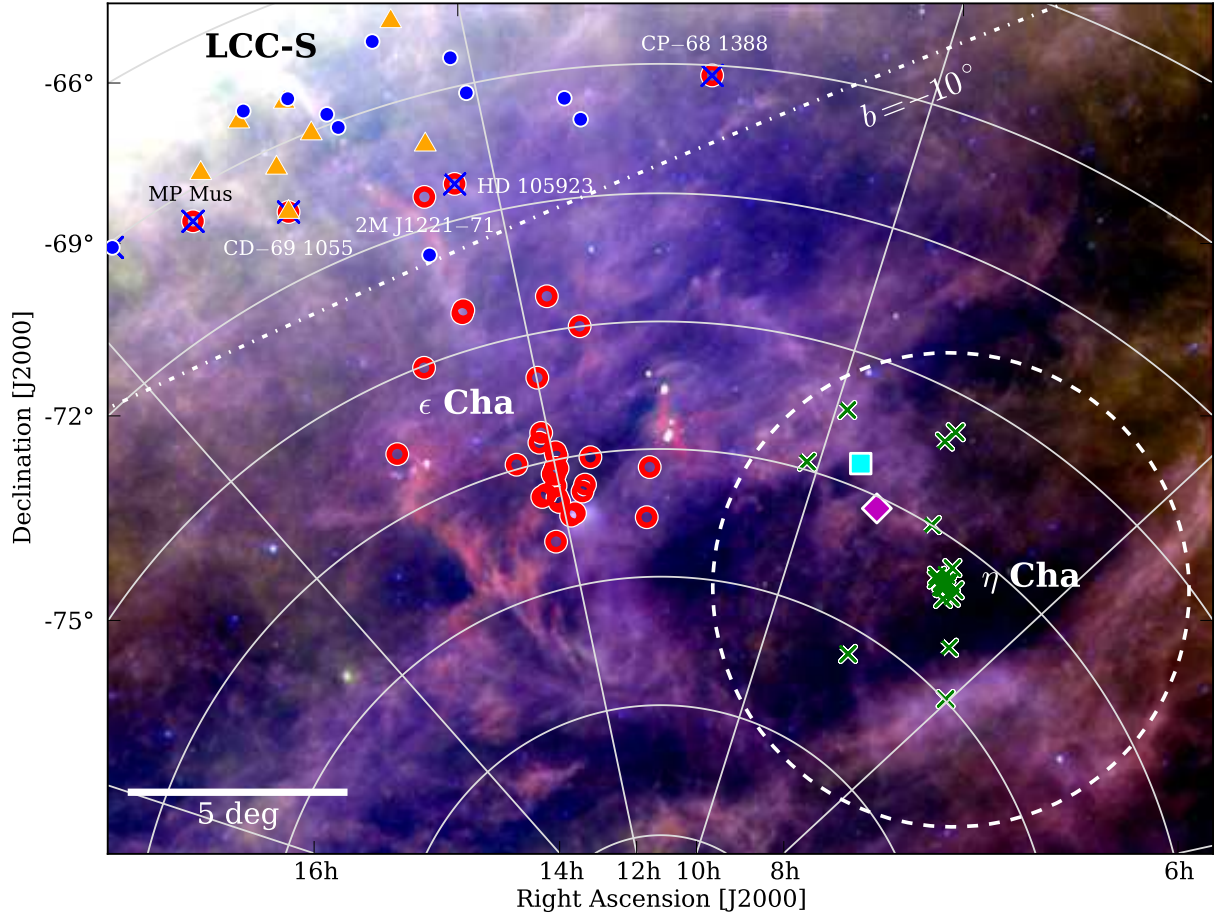


Figure 22. *IRAS* colour map with η Cha members (green crosses) and confirmed or provisional members of ϵ Cha (open circles). Stars discussed in the text are labelled. The diamond and square are the wide systems HD 82879/82859 and RX J0942.7-7726AB, respectively. LCC members from Mamajek et al. (2002) (blue crosses), de Zeeuw et al. (1999) (filled circles) and Song et al. (2012) (triangles) are shown with the $b = -10^\circ$ ‘boundary’ of the subgroup (dot dashed line). The dashed line is the 5.5 deg radius around η Cha surveyed for new members by Murphy et al. (2010).

Table 10. Observed and predicted kinematics of northern ϵ Cha/LCC members

MML ID*	Star	Observed		RV [‡] [km s ⁻¹]	ϵ Cha		d_{kin} [pc]	LCC (Chen et al. 2011)		RV [km s ⁻¹]	d_{kin} [pc]	Memb.?
		$(\mu_\alpha \cos \delta, \mu_\delta)^\dagger$ [mas yr ⁻¹]			$(\mu_\alpha \cos \delta, \mu_\delta)$ [mas yr ⁻¹]			$(\mu_\alpha \cos \delta, \mu_\delta)$ [mas yr ⁻¹]				
	2M J1221-71	-39.4	-11.8	11.5	-39	-11	13.4	-42	-4	14.6	89	ϵ Cha
1	CP-68 1388	-36.1	+5.7	15.9	-37	+2	15.8	-36	+8	16.7	91	LCC?
7	HD 105923	-38.9	-8.3	14.2	-39	-9	13.7	-40	-3	14.9	92	ϵ Cha
27	CD-69 1055	-43.1	-18.7	12.8	-43	-19	12.2	-46	-12	13.6	82	ϵ Cha
34	MP Mus	-40.8	-23.3	11.6	-41	-23	11.4	-45	-17	12.9	84	ϵ Cha

(*) Identifier from Mamajek, Meyer & Liebert (2002)

(†) Proper motions from Tycho-2 and SPM4 (2MASS J12210499-7116493)

(‡) Radial velocities from Torres et al. (2006) and Kiss et al. (2011) (2MASS J12210499-7116493)

than GKM-type LCC members recently proposed by Song et al. (2012) (or the roughly coeval β Pic). Pending better knowledge of the low-mass population of southern LCC, all five stars are likely members of ϵ Cha as defined in this study.

However, given their similar ages, locations and distances a useful demarcation between the southern extent of LCC and ϵ Cha may not exist. Recent surveys (Song et al. 2012; Rodriguez et al. 2011) have already identified many young stars immediately north

of ϵ Cha (Fig. 22) and the provisional candidate RX J1202.8-7718 may be a dispersed LCC member juxtaposed on the central region of ϵ Cha. A similar problem exists at the northern boundary of LCC and TW Hya, where young stars at 70–150 pc have ambiguous memberships (Mamajek 2005). Clarifying this messy picture of star formation will require a larger sample of young stars around Sco-Cen with reliable distances and ages. The *Gaia* astrometric satellite will help immensely in this regard.

In the interim we can only speculate how η and ϵ Cha formed within the greater Sco-Cen region. A schematic picture was provided by Feigelson (1996), who proposed young stars born in different parts of a dynamically unbound giant molecular cloud (GMC) are dispersed by internal turbulent velocities. In this picture some parts of the GMC may collapse quickly to form rich clusters while other regions remain stable against collapse as they disperse, forming stellar aggregates of a range of ages and sizes over wide areas. Preibisch & Mamajek (2008) proposed that the bulk of star formation in UCL and LCC probably proceeded in this way as a series of small clusters and filaments, each containing tens to hundreds of stars. The local virial balance of the nascent cloudlets meant some resulting young groups are compact (η Cha and the core of ϵ Cha), while others appear unbound and widely dispersed (e.g. TW Hya, β Pic and the outer members of ϵ Cha) (Feigelson et al. 2003).

9 SUMMARY

We have critically re-examined membership of the young ϵ Cha association using the best-available spectroscopic and kinematic measurements. The main results of this study are:

- Of the 52 candidates proposed in the literature we confirm 35 stars as members of ϵ Cha, with spectral types of B9 to mid-M. Six candidates are classified as provisional members requiring better kinematics or distances.

- ϵ Cha lies at a mean distance of 110 ± 7 pc and has a mean space motion of $(U, V, W) = (-10.9 \pm 0.8, -20.4 \pm 1.3, -9.9 \pm 1.4)$ km s⁻¹. Comparison of its HR diagram to theoretical evolutionary models suggests ϵ Cha is 3–5 Myr old, distinguishing it as the youngest kinematic group in the solar neighbourhood and the only one associated with remnant molecular material.

- Fifteen members have infrared spectral energy distributions attributable to circumstellar discs, including 11 stars which are actively accreting material. As expected of an intermediate-age population they show a variety of morphologies, from optically-thick accretion discs, to weak-excess debris discs.

- After considering all the available observations we rejected several proposed members. They instead belong to the background Cha I and II cloud populations and other nearby young groups. In the absence of parallaxes and precise stellar ages we emphasise the importance of a holistic and conservative approach to assigning stars to kinematic groups, many of which have only subtly different properties and ill-defined memberships.

- A comparative age analysis shows that ϵ Cha is approximately 1–3 Myr younger than the nearby η Cha open cluster. Contrary to earlier studies which assumed η and ϵ Cha are coeval and formed in the same location, we find the groups were separated by ~ 30 pc when η Cha was born, followed soon after by ϵ Cha.

- The physical properties, locations and kinematics of η and ϵ Cha are consistent with them being formed in the turbulent ISM surrounding the Scorpius-Centaurus OB association. They are likely products of the last burst of star formation in southern Sco-Cen, which earlier formed the sparse TW Hya and β Pic groups and several thousand older (now field) stars.

ACKNOWLEDGMENTS

We thank Pavel Kroupa, Eric Mamajek and Eric Feigelson for their considered comments on the thesis of SJM from which this work is based, and the anonymous referee for their thorough review

of the manuscript. We also thank the ANU TAC for their generous allocation of telescope time. This research has made extensive use of the VizieR and SIMBAD services provided by CDS, Strasbourg and the TOPCAT software package developed by Mark Taylor (U. Bristol). Many catalogues used in this work are hosted by the German Astrophysical Virtual Observatory. *WISE* is a joint project of the University of California, Los Angeles, and the Jet Propulsion Laboratory/California Institute of Technology, funded by NASA. 2MASS is a joint project of the University of Massachusetts and the Infrared Processing and Analysis Centre/California Institute of Technology, funded by NASA and the NSF.

REFERENCES

- Alcala J. M., Krautter J., Schmitt J. H. M. M., Covino E., Wichmann R., Mundt R., 1995, *A&AS*, 114, 109
- Appenzeller I., Mundt R., 1989, *A&A Rev.*, 1, 291
- Baraffe I., Chabrier G., 2010, *A&A*, 521, A44
- Barbier-Brossat M., Figon P., 2000, *A&AS*, 142, 217
- Barrado y Navascues D., 1998, *A&A*, 339, 831
- Becker C., Moraux E., Duchêne G., Maschberger T., Lawson W., 2013, *A&A*, 552, A46
- Bessell M. S., Brett J. M., 1988, *PASP*, 100, 1134
- Böhm T., Catala C., Balona L., Carter B., 2004, *A&A*, 427, 907
- Brandeker A., Liseau R., Artymowicz P., Jayawardhana R., 2001, *ApJ*, 561, L199
- Brandeker A., Jayawardhana R., Khavari P., Haisch Jr. K. E., Mardones D., 2006, *ApJ*, 652, 1572
- Cameron E., 2011, *PASA*, 28, 128
- Carpenter J. M., 2001, *AJ*, 121, 2851
- Chen C. H., Mamajek E. E., Bitner M. A., Pecaut M., Su K. Y. L., Weinberger A. J., 2011, *ApJ*, 738, 122
- Cohen M., Wheaton W. A., Megeath S. T., 2003, *AJ*, 126, 1090
- Correia S., Zinnecker H., Ratzka T., Sterzik M. F., 2006, *A&A*, 459, 909
- Covino E., Alcala J. M., Allain S., Bouvier J., Terranegra L., Krautter J., 1997, *A&A*, 328, 187
- Currie T., Thalmann C., Matsumura S., Madhusudhan N., Burrows A., Kuchner M., 2011, *ApJ*, 736, L33
- Cutispoto G., Pastori L., Pasquini L., de Medeiros J. R., Tagliaferri G., Andersen J., 2002, *A&A*, 384, 491
- da Silva L., Torres C. A. O., de La Reza R., Quast G. R., Melo C. H. F., Sterzik M. F., 2009, *A&A*, 508, 833
- de Zeeuw P. T., Hoogerwerf R., de Bruijne J. H. J., Brown A. G. A., Blaauw A., 1999, *AJ*, 117, 354
- Dopita M., Hart J., McGregor P., Oates P., Bloxham G., Jones D., 2007, *Ap&SS*, 310, 255
- Dotter A., Chaboyer B., Jevremović D., Kostov V., Baron E., Ferguson J. W., 2008, *ApJS*, 178, 89
- Ducourant C., Teixeira R., Périé J. P., Lecampion J. F., Guibert J., Sartori M. J., 2005, *A&A*, 438, 769
- Epchtein N. et al., 1999, *A&A*, 349, 236
- Fang M., van Boekel R., Wang W., Carmona A., Sicilia-Aguilar A., Henning T., 2009, *A&A*, 504, 461
- Fang M., van Boekel R., Bouwman J., Henning T., Lawson W. A., Sicilia-Aguilar A., 2013, *A&A*, 549, A15
- Fedele D., van den Ancker M. E., Henning T., Jayawardhana R., Oliveira J. M., 2010, *A&A*, 510, A72
- Feigelson E. D., 1996, *ApJ*, 468, 306
- Feigelson E. D., Lawson W. A., Garmire G. P., 2003, *ApJ*, 599, 1207
- Fouqué P. et al., 2000, *A&AS*, 141, 313
- Franchini M., Covino E., Stalio R., Terranegra L., Chavarria-K. C., 1992, *A&A*, 256, 525
- Frink S., Roeser S., Alcala J. M., Covino E., Brandner W., 1998, *A&A*, 338, 442
- Girard T. M. et al., 2011, *AJ*, 142, 15
- Grady C. A. et al., 2004, *ApJ*, 608, 809

- Grenier S., Burnage R., Faraggiana R., Gerbaldi M., Delmas F., Gómez A. E., Sabas V., Sharif L., 1999, *A&AS*, 135, 503
- Guenther E. W., Esposito M., Mundt R., Covino E., Alcalá J. M., Cusano F., Stecklum B., 2007, *A&A*, 467, 1147
- Gustafsson B., Edvardsson B., Eriksson K., Jørgensen U. G., Nordlund Å., Plez B., 2008, *A&A*, 486, 951
- Høg E. et al., 2000, *A&A*, 355, L27
- James D. J., Melo C., Santos N. C., Bouvier J., 2006, *A&A*, 446, 971
- Jarrett T. H. et al., 2011, *ApJ*, 735, 112
- Jayawardhana R., Mohanty S., Basri G., 2003, *ApJ*, 592, 282
- Jilinski E., Ortega V. G., de la Reza R., 2005, *ApJ*, 619, 945
- Kastner J. H., Thompson E. A., Montez R., Murphy S. J., Bessell M. S., Sacco G., 2012, *ApJ*, 747, L23
- Kenyon S. J., Hartmann L., 1995, *ApJS*, 101, 117
- Kiss L. L. et al., 2011, *MNRAS*, 411, 117
- Knee L. B. G., Prusti T., 1996, *A&A*, 312, 455
- Knude J., 2010, *ArXiv e-prints*: astro-ph/1006.3676
- Knude J., Hog E., 1998, *A&A*, 338, 897
- Köhler R., 2001, *AJ*, 122, 3325
- Kraus A. L., Hillenbrand L. A., 2007, *AJ*, 134, 2340
- Lawson W. A., Lyo A. R., Muzerolle J., 2004, *MNRAS*, 351, L39
- Lawson W. A., Lyo A., Bessell M. S., 2009, *MNRAS*, 400, L29
- Lopez Martí B., Jimenez Esteban F., Bayo A., Barrado D., Solano E., Rodrigo C., 2013, *A&A*, 551, A46
- Luhman K. L., 2004a, *ApJ*, 602, 816
- Luhman K. L., 2004b, *ApJ*, 616, 1033
- Luhman K. L., 2007, *ApJS*, 173, 104
- Luhman K. L., 2008, *Handbook of Star Forming Regions*, Vol. II: The Southern Sky, ASP Press. p. 169
- Luhman K. L., Steeghs D., 2004, *ApJ*, 609, 917
- Luhman K. L., Stauffer J. R., Muench A. A., Rieke G. H., Lada E. A., Bouvier J., Lada C. J., 2003, *ApJ*, 593, 1093
- Luhman K. L., Allen P. R., Espaillat C., Hartmann L., Calvet N., 2010, *ApJS*, 186, 111
- Luhman K. L. et al., 2008, *ApJ*, 675, 1375
- Lyo A. R., Lawson W. A., Bessell M. S., 2004a, *MNRAS*, 355, 363
- Lyo A. R., Lawson W. A., Feigelson E. D., Crause L. A., 2004b, *MNRAS*, 347, 246
- Lyo A. R., Lawson W. A., Bessell M. S., 2008, *MNRAS*, 389, 1461
- Makarov V. V., Olling R. P., Teuben P. J., 2004, *MNRAS*, 352, 1199
- Malo L., Doyon R., Lafrenière D., Artigau É., Gagné J., Baron F., Riedel A., 2013, *ApJ*, 762, 88
- Mamajek E. E., 2005, *ApJ*, 634, 1385
- Mamajek E. E., Feigelson E. D., 2001, in R. Jayawardhana, T. Greene, eds, *Young Stars Near Earth: Progress and Prospects*. Astronomical Society of the Pacific Conference Series, Vol. 244, pp. 104–115
- Mamajek E. E., Lawson W. A., Feigelson E. D., 1999, *ApJ*, 516, L77
- Mamajek E. E., Lawson W. A., Feigelson E. D., 2000, *ApJ*, 544, 356
- Mamajek E. E., Meyer M. R., Liebert J., 2002, *AJ*, 124, 1670
- Manoj P. et al., 2011, *ApJS*, 193, 11
- Mentuch E., Brandeker A., van Kerkwijk M. H., Jayawardhana R., Hauschildt P. H., 2008, *ApJ*, 689, 1127
- Mizuno A. et al., 1998, *ApJ*, 507, L83
- Murphy S. J., Lawson W. A., Bessell M. S., 2010, *MNRAS*, 406, L50
- Murphy S. J., Lawson W. A., Bessell M. S., Bayliss D. D. R., 2011, *MNRAS*, 411, L51
- Murphy S. J., Lawson W. A., Bessell M. S., 2012, *MNRAS*, 424, 625
- Muzerolle J., Calvet N., Briceño C., Hartmann L., Hillenbrand L., 2000, *ApJ*, 535, L47
- Nakajima T., Morino J. I., 2012, *AJ*, 143, 2
- Natta A., Testi L., Muzerolle J., Randich S., Comerón F., Persi P., 2004, *A&A*, 424, 603
- Nordström B. et al., 2004, *A&A*, 418, 989
- Perryman M. A. C. et al., 1997, *A&A*, 323, L49
- Pickles A. J., 1998, *PASP*, 110, 863
- Preibisch T., Mamajek E. E., 2008, *Handbook of Star Forming Regions*, Vol. II. The Southern Sky, ASP Press. p. 235
- Riaz B., Gizis J. E., Harvin J., 2006, *AJ*, 132, 866
- Riddick F. C., Roche P. F., Lucas P. W., 2007, *MNRAS*, 381, 1067
- Rodriguez D. R., Bessell M. S., Zuckerman B., Kastner J. H., 2011, *ApJ*, 727, 62
- Röser S., Demleitner M., Schilbach E., 2010, *AJ*, 139, 2440
- Schisano E., Covino E., Alcalá J. M., Esposito M., Gandolfi D., Guenther E. W., 2009, *A&A*, 501, 1013
- Schlegel D. J., Finkbeiner D. P., Davis M., 1998, *ApJ*, 500, 525
- Shkolnik E., Liu M. C., Reid I. N., 2009, *ApJ*, 699, 649
- Sicilia-Aguilar A. et al., 2009, *ApJ*, 701, 1188
- Siess L., Dufour E., Forestini M., 2000, *A&A*, 358, 593
- Simon M., Schlieder J. E., Constantin A. M., Silverstein M., 2012, *ApJ*, 751, 114
- Skrutskie M. F. et al., 2006, *AJ*, 131, 1163
- Song I., Zuckerman B., Bessell M. S., 2012, *AJ*, 144, 8
- Spezzi L. et al., 2008, *ApJ*, 680, 1295
- Terranegra L., Morale F., Spagna A., Massone G., Lattanzi M. G., 1999, *A&A*, 341, L79
- Torres C. A. O., Quast G. R., da Silva L., de La Reza R., Melo C. H. F., Sterzik M., 2006, *A&A*, 460, 695
- Torres C. A. O., Quast G. R., Melo C. H. F., Sterzik M. F., 2008, *Handbook of Star Forming Regions*, Vol. II: The Southern Sky, ASP Press. p. 757
- van Leeuwen F., 2007, *A&A*, 474, 653
- Wahhaj Z. et al., 2010, *ApJ*, 724, 835
- Wichmann R., Schmitt J. H. M. M., Hubrig S., 2003, *A&A*, 399, 983
- Williams J. P., Cieza L. A., 2011, *ARA&A*, 49, 67
- Wright E. L. et al., 2010, *AJ*, 140, 1868
- Zacharias N., Finch C. T., Girard T. M., Henden A., Bartlett J. L., Monet D. G., Zacharias M. I., 2013, *AJ*, 145, 44
- Zboril M., Byrne P. B., Rolleston W. R. J. R., 1997, *MNRAS*, 284, 685
- Zuckerman B., Song I., 2004, *ARA&A*, 42, 685

APPENDIX A: FINDING CHARTS

Finding charts for RX J1150.9–7411 ($11^{\text{h}}50^{\text{m}}45.2^{\text{s}}$, $-74^{\circ}11'13''$, J2000) and RX J1243.1–7458 ($12^{\text{h}}42^{\text{m}}53.0^{\text{s}}$, $-74^{\circ}58'49''$, J2000) are shown in Fig. A1. Lower-resolution charts with the correct source identifications were presented by Alcalá et al. (1995). However, for RX J1150.9–7411 and RX J1243.1–7458 the coordinates in that study were incorrect.

APPENDIX B: CANDIDATE INFORMATION

The astrometric and spectroscopic measurements adopted for each candidate are listed in Table B1 with appropriate references. Near-infrared photometry from DENIS, 2MASS and *WISE* is given in Table B2.

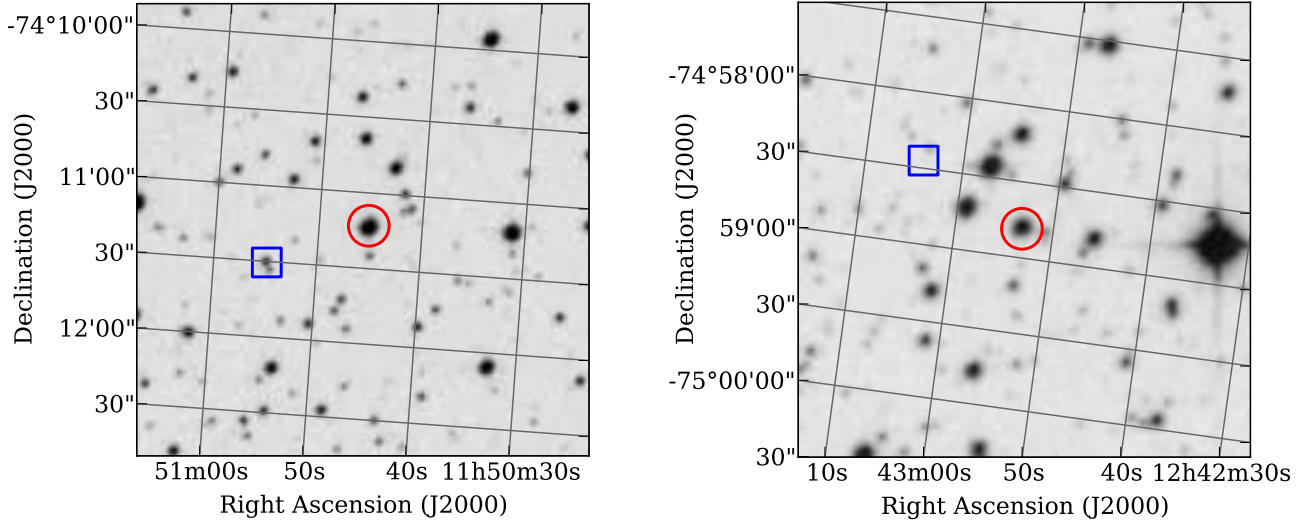


Figure A1. POSS2-Red finding charts for RX J1150.9–7411 (left) and RX J1243.1–7458 (right). The new optical positions are circled, while the incorrect Alcala et al. (1995) positions are shown as blue squares.

Table B1. Adopted astrometry and spectroscopic measurements of ϵ Cha candidates. Spectral types, velocities and equivalent width measurements are derived from our WiFeS spectroscopy unless specified.

(‡) References: (T06) Torres et al. (2006), (T08) Torres et al. (2008), (L04) Luhman (2004b), (LL04) Luhman (2004a), (ZS04) Zuckerman & Song (2004), (K12) Kastner et al. (2012), (M00) Mamajek et al. (2000), (R06) Riaz et al. (2006), (C97) Covino et al. (1997), (G07) Guenther et al. (2007), (N04) Nordström et al. (2004), (TCha) Same velocity as T Cha, (J06) James et al. (2006), (G99) Grenier et al. (1999), (BB00) Barbier-Brossat & Figon (2000), (G04) Grady et al. (2004), (K11) Kiss et al. (2011), (dS09) da Silva et al. (2009), (M11) Manoj et al. (2011), (S09) Schisano et al. (2009), (F03) Feigelson et al. (2003), (S08) Spezzi et al. (2008).

(†) Proper motion references: (TYC) Tycho-2/Høg et al. (2000), (HIP) *Hipparcos*/van Leeuwen (2007), (UCAC4) Zacharias et al. (2013), (SPM4) Girard et al. (2011), (PPMXL) Röser et al. (2010).

Table B2. Adopted photometry for ϵ Cha candidates. Unless specified, I -band data is from the DENIS survey (Epchtein et al. 1999) with JHK_s from 2MASS (Skrutskie et al. 2006) and $W1, W2, W3, W4$ from WISE (Wright et al. 2010).

ID	Name	I [mag]	Ref. [‡]	J [mag]	H [mag]	K_s [mag]	Ref. [‡]	$W1$ [mag]	$W2$ [mag]	$W3$ [mag]	$W4$ [mag]
	HD 82879	8.95		8.12	7.93	7.83		7.78	7.80	7.82	7.92
	CP-68 1388	9.28	T06	8.48	8.01	7.79		7.72	7.74	7.68	7.59
	VW Cha	11.03	B01	8.70	7.64	6.96		6.15	5.40	4.12	1.85
	TYC 9414-191-1	9.59		8.41	7.76	7.53		7.43	7.55	7.45	7.43
13	2MASS J11183572-7935548	12.22		10.49	9.89	9.62		9.42	9.14	7.67	4.47
14	RX J1123.2-7924	11.62		10.52	9.84	9.67		9.52	9.46	9.31	8.61
	HIP 55746	7.15	†	6.73	6.57	6.49		6.40	6.44	6.46	6.41
15	2MASS J11334926-7618399	14.08		12.15	11.50	11.18		11.08	10.86	10.72	8.90
	RX J1137.4-7648	12.20	#	11.85	10.48	10.14		9.80	9.70	9.59	8.94
16	2MASS J11404967-7459394	15.02		12.68	12.15	11.77		11.58	11.31	11.04	9.31
	TYC 9238-612-1	9.98		9.39	9.02	8.86		8.78	8.80	8.74	8.49
17	2MASS J11432669-7804454	13.51		11.62	10.97	10.60		10.23	9.84	8.71	7.12
	RX J1147.7-7842	10.92		9.52	8.86	8.59		8.47	8.33	8.22	8.42
18	RX J1149.8-7850	11.01		9.45	8.72	8.49		8.20	7.67	4.54	1.82
19	RX J1150.4-7704	10.54		9.71	9.13	8.97		8.86	8.87	8.79	8.71
	RX J1150.9-7411	12.06	†	10.60	9.78	9.48		9.31	9.14	8.98	8.64
	2MASS J11550485-7919108	13.26		11.22	10.46	10.08		9.87	9.65	9.27	6.84
	T Cha	10.28		8.96	7.86	6.95		5.84	5.01	4.66	2.56
20	RX J1158.5-7754B	11.81		10.34	9.71	9.44		9.35	9.20	9.08	8.75
21	RX J1158.5-7754A	9.76	†	8.63	7.56	7.40		7.27	7.28	7.19	7.08
	HD 104036	6.49	HIP	6.29	6.22	6.11		6.10	6.08	6.13	6.08
1	CXOU J115908.2-781232	13.83	F03	12.01	11.45	11.17		10.97	10.74	10.19	8.32
2	ϵ Cha A	5.39	F03*	5.52	5.04	4.98		5.25	4.97	5.11	4.84
	RX J1159.7-7601	10.18		9.14	8.47	8.30		8.16	8.19	8.08	7.85
3	HD 104237C	15.28	14.85	14.48	G04
4	HD 104237B	11.43	10.27	9.52	G04
5	HD 104237A	6.31	HIP	5.81	5.25	4.58		3.89	2.47	0.93	-0.91
6	HD 104237D	11.62	F03	10.53	9.73	9.67	G04
7	HD 104237E	10.28	F03	9.10	8.05	7.70	G04
10	2MASS J12005517-7820296	14.00		11.96	11.40	11.01		10.62	10.16	8.52	6.61
	HD 104467	7.81	T06	7.26	6.97	6.85		6.81	6.80	6.78	6.82
11	2MASS J12014343-7835472	15.96		14.36	13.38	12.81		12.36	11.60	7.59	5.24
8	USNO-B 120144.7-781926	13.72	F03	11.68	11.12	10.78		10.16	9.74	8.35	6.70
9	CXOU J120152.8-781840	13.52	F03	11.63	11.04	10.77		10.57	10.35	10.05	9.32
	RX J1202.1-7853	10.49		9.21	8.46	8.31		8.10	8.04	7.92	8.13
	RX J1202.8-7718	11.90		10.51	9.82	9.59		9.53	9.40	9.20	8.78
	RX J1204.6-7731	11.25		9.77	9.12	8.88		8.74	8.59	8.50	8.81
	TYC 9420-676-1	9.73		9.24	9.09	8.94		8.86	8.88	8.86	9.15
	HD 105234	7.17	HIP	6.87	6.76	6.68		6.55	6.48	5.43	4.57
12	2MASS J12074597-7816064	13.11		11.55	10.98	10.67		10.50	10.33	10.19	8.88
	RX J1207.7-7953	12.06		10.43	9.76	9.57		9.45	9.31	9.24	8.62
	HIP 59243	6.56	HIP	6.34	6.23	6.17		6.11	6.12	6.16	6.05
	HD 105923	8.31	T06	7.67	7.31	7.17		7.07	7.08	7.04	6.96
	RX J1216.8-7753	11.65		10.09	9.46	9.24		9.14	9.03	8.91	8.76
	RX J1219.7-7403	10.95		9.75	9.05	8.86		8.75	8.67	8.54	8.28
	RX J1220.4-7407	10.80	†	9.43	8.61	8.37		8.26	8.15	8.04	8.11
	2MASS J12210499-7116493	10.21		9.09	8.42	8.24		8.16	8.16	8.08	7.99
	RX J1239.4-7502	9.21	T06	8.43	7.95	7.78		7.72	7.75	7.71	7.45
	RX J1243.1-7458	12.72	†	11.27	10.15	9.81		9.54	9.37	9.34	9.48
	CD-69 1055	8.89	T06	8.18	7.70	7.54		7.43	7.47	7.42	7.44
	CM Cha	11.80	T06	10.02	9.16	8.52		7.62	7.16	5.06	3.06
	MP Mus	9.18	T06	8.28	7.64	7.29		6.58	6.18	4.06	1.59

(‡) Photometry references: (T06) SACY/Torres et al. (2006), (HIP) *Hipparcos* catalogue (Perryman et al. 1997), (F03) Feigelson et al. (2003), (G04) Grady et al. (2004), (B01) Brandeker et al. (2001).

(†) DENIS I and 2MASS J photometry corrected for multiplicity using the K -band flux ratios of Köhler (2001) and main-sequence colours of Kraus & Hillenbrand (2007).

(*) F03 I and 2MASS J photometry corrected for multiplicity using the V -band magnitudes in Feigelson et al. (2003) and main-sequence colours of Kraus & Hillenbrand (2007).

(#) DENIS I and 2MASS J photometry corrected assuming an equal-mass system.